

1 Plasma concentrations of organohalogenated contaminants in white-tailed eagle
2 nestlings – The role of age and diet

3 Mari Engvig Løseth^{a*}, Nathalie Briels^a, Igor Eulaers^b, Torgeir Nygård^c, Govindan
4 Malarvannan^d, Giulia Poma^d, Adrian Covaci^d, Dorte Herzke^e, Jan Ove Bustnes^f, Gilles
5 Lepoint^g, Bjørn Munro Jenssen^{a,b}, Veerle L. B. Jaspers^a

6

7 ^aDepartment of Biology, Norwegian University of Science and Technology (NTNU),
8 Høgskoleringen 5, 7491 Trondheim, Norway

9 ^bDepartment of Bioscience, Aarhus University, Fredriksborgvej 399, 4000 Roskilde,
10 Denmark

11 ^cNorwegian Institute for Nature Research (NINA), Høgskoleringen 9, 7034 Trondheim,
12 Norway

13 ^dToxicological Centre, University of Antwerp, Universiteitsplein 1, 2610 Wilrijk, Belgium

14 ^eNorwegian Institute for Air Research (NILU), FRAM - High North Research Centre on
15 Climate and the Environment, 9007 Tromsø, Norway

16 ^fNorwegian Institute for Nature Research (NINA), FRAM - High North Research Centre on
17 Climate and the Environment, 9007 Tromsø, Norway

18 ^gLaboratoire d'Océanologie, University of Liège, 4000 Liège (Sart-Tilman), Belgium

19 * Corresponding author: mari.loseth@ntnu.no

20

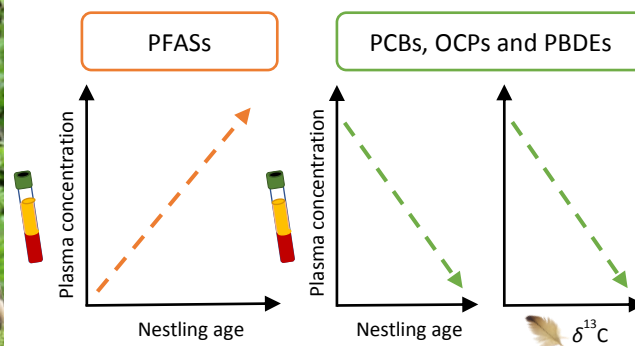
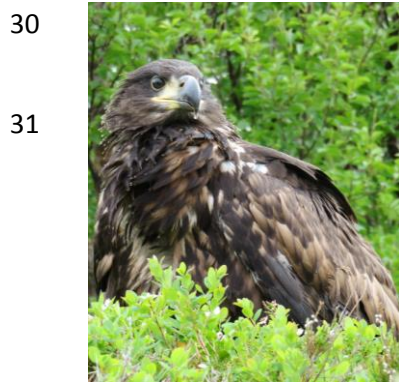
21 Highlights:

- 22 • Significant temporal and spatial variations were found for all compound groups
- 23 • Age was the most important predictor for contaminant variation in nestling plasma
- 24 • Concentrations of legacy PCBs, OCPs and PBDEs decreased with age
- 25 • Concentrations of PFASs increased with age
- 26 • $\delta^{13}\text{C}$ significantly predicted the variation of legacy PCBs, OCPs and PBDEs

27 Keywords:

28 Temporal; spatial; growth dilution; stable isotopes; *Haliaeetus albicilla*; pollution

29 Graphical abstract



32 Abstract

33 Concentrations of organohalogenated contaminants (OHCs) can show significant temporal
34 and spatial variation in the environment and wildlife. Most of the variation is due to changes
35 in use and production, but environmental and biological factors may also contribute to the
36 variation. Nestlings of top predators are exposed to maternally transferred OHCs in the egg
37 and through their dietary intake after hatching. The present study investigated spatial and
38 temporal variation of OHCs and the role of age and diet on these variations in plasma from
39 Norwegian white-tailed eagle (*Haliaeetus albicilla*) nestlings. The nestlings were sampled at
40 two locations, Smøla and Steigen, in 2015 and 2016. The age of the nestlings was recorded
41 (range: 44 – 87 days old) and stable carbon and nitrogen isotopes ($\delta^{13}\text{C}$ and $\delta^{15}\text{N}$) were
42 applied as dietary proxies for carbon source and trophic position, respectively. In total, 14
43 polychlorinated biphenyls (PCBs, range: 0.82 – 59.05 ng/mL), 7 organochlorinated pesticides
44 (OCPs, range: 0.89 – 52.19 ng/mL), 5 polybrominated diphenyl ethers (PBDEs, range: 0.03 –
45 2.64 ng/mL) and 8 perfluoroalkyl substances (PFASs, range: 4.58 – 52.94 ng/mL) were
46 quantified in plasma samples from each location and year. The OHC concentrations, age and
47 dietary proxies displayed temporal and spatial variations. The age of the nestlings was
48 indicated as the most important predictor for OHC variation as the models displayed
49 significantly decreasing plasma concentrations of PCBs, OCPs, and PBDEs with increasing
50 age, while concentrations of PFASs were significantly increasing with age. Together with
51 age, the variations in PCB, OCP and PBDE concentrations were also explained by $\delta^{13}\text{C}$ and
52 indicated decreasing concentrations with a more marine diet. Our findings emphasise age and
53 diet as important factors to consider when investigating variations in plasma OHC
54 concentrations in nestlings.

55

56 1. Introduction

57 Organohalogenated contaminants (OHCs) are a diverse group of chemicals that have been
58 used in lubricants, pesticides, flame retardants and surface treatments (Mackay et al., 2006).
59 OHCs include legacy compounds such as polychlorinated biphenyls (PCBs), as well as
60 emerging compounds such as per- and polyfluoroalkyl substances (PFASs). By being
61 resistant to chemical and biological degradation, OHCs persist in the environment (Muir and
62 de Wit, 2010; UNEP, 2009). While most legacy OHCs are lipophilic, the emerging PFASs
63 are amphipathic due to a different chemical structure with a hydrophilic functional group
64 (Lau et al., 2007) . Even so, their physicochemical properties and persistency result in high
65 potential for bioaccumulation and biomagnification through food chains (Borgå et al., 2004,
66 2012). The concentrations of OHCs can show significant temporal and spatial variations both
67 in the environment and wildlife (Faxneld et al., 2016; Helgason et al., 2008; Hung et al.,
68 2016; Wierda et al., 2016). Most of these variations are due to changes in production and use
69 of the compounds (Hung et al., 2016; Wang et al., 2014). However, environmental and
70 biological factors can also contribute significantly to the observed variations (Bourgeon et al.,
71 2013; Bustnes et al., 2015; Leat et al., 2011).

72 The white-tailed eagle (*Haliaeetus albicilla*) occupies a high trophic level and can
73 accumulate a wide range of OHCs, even at an early age (Bustnes et al., 2013; Eulaers et al.,
74 2014; Løseth et al., 2019; Sletten et al., 2016). Nestlings are exposed to maternally
75 transferred OHCs during development in the egg (Faxneld et al., 2016; Nordlöf et al., 2010;
76 Nygård and Polder, 2012) and the exposure continues after hatching through their dietary
77 intake (Bourgeon et al., 2013). Adult white-tailed eagles are mostly resident within their
78 breeding areas (Willgohs, 1984), thus the contaminant burdens of their eggs and nestlings
79 reflect contaminant levels in local prey. This makes white-tailed eagle nestlings good
80 sentinels of local environmental pollution (Helander et al., 2008; Olsson et al., 2000).

81 The diet of the white-tailed eagle consists mainly of marine fish and seabirds (Koivusaari et
82 al., 1976; Willgohs, 1984), which may have accumulated high concentrations of OHCs. As
83 the diet is a major source of OHC exposure following hatching, stable isotopes of nitrogen
84 ($\delta^{15}\text{N}$) and carbon ($\delta^{13}\text{C}$) are often applied as dietary proxies to investigate the nestlings'
85 trophic position and dietary carbon source, respectively (Fry, 2006; Inger and Bearhop,
86 2008). The ratio of ^{15}N to ^{14}N increases by about 2-5 ‰ per trophic level as the lighter
87 nitrogen isotopes are excreted through nitrogenous waste products. The ratio of ^{13}C to ^{12}C can
88 also increase with increasing trophic level, though it is mostly used to distinguish between
89 marine and terrestrial dietary carbon sources. Terrestrial primary producers have lower $\delta^{13}\text{C}$
90 values compared to marine ones. This is reflected in the tissues of their consumers and
91 persists at higher trophic levels within the food chain (Fry, 2006; Inger and Bearhop, 2008;
92 Kelly, 2000). Keratinized matrices, such as feathers, are metabolically inert after their growth
93 and can preserve the stable isotopes deposited into the matrix during its growth (Inger and
94 Bearhop, 2008). A homogenate of nestling feathers can therefore provide information about
95 their diet during the growth period of the feathers (Bearhop et al., 2002).

96 As many OHCs have been shown to interfere with physiological processes linked to
97 development and growth (Cassone et al., 2012; Jenssen et al., 2010; Nøst et al., 2012), there
98 is special concern about levels and effects of these compounds in young developing birds. As
99 nestlings develop and grow, their maternally transferred contaminants are significantly
100 diluted by their growth (Bourgeon et al., 2013; Bustnes et al., 2013). However, nestlings are
101 also exposed to OHCs through their diet and plasma concentrations of compounds with high
102 ability for bioaccumulation may increase as the nestlings reach their adult body size at
103 fledging (Borgå et al., 2004; Bustnes et al., 2013). Previously, only few studies have
104 accounted for age and growth when investigating OHCs in nestlings (Bourgeon et al., 2013;
105 Bustnes et al., 2013; Dauwe et al., 2006; Olsson et al., 2000). In the present study, we aimed

106 to investigate variations of OHC concentrations in plasma from white-tailed eagle nestlings
107 sampled from two locations in two consecutive years. Secondly, we aimed to explore if
108 variation in dietary proxies ($\delta^{13}\text{C}$ and $\delta^{15}\text{N}$) and biological variables (such as age of the
109 nestlings) could account for parts of the spatial and temporal variation of these OHCs. As the
110 diet is the major source of OHCs, we expected to find a strong influence of the dietary
111 proxies presenting increased plasma OHCs with increasing $\delta^{15}\text{N}$ (higher trophic position) and
112 increasing $\delta^{13}\text{C}$ (more marine prey). Thus, we also expected to find small differences in
113 OHCs in nestlings from the two locations as habitat differences may also influence the
114 diversity of prey species at the two locations. No differences were expected between the two
115 sampling years, as to the authors knowledge there are no local sources of OHCs at the two
116 locations. We also expected to find higher concentrations in plasma of older and/or larger
117 nestlings as OHCs have a high potential for bioaccumulation.

118 2. Materials and methods

119 The plasma OHC concentrations of the individual OHCs have been published previously
120 (Løseth et al., 2019, supplementary information), in a study where three non-invasive
121 matrices (plasma, feathers and preen oil) from white-tailed eagle nestlings were compared for
122 legacy and emerging contaminants. In the current study, however, we present unpublished
123 data on stable isotopes and age to explain variation in the plasma concentrations of ΣPCBs ,
124 ΣOCPs , ΣPBDEs and ΣPFASs .

125 2.1. Field sampling

126 The study was conducted on 70 white-tailed eagle nestlings from two archipelagos in
127 Norway, Smøla (63.3-63.5°N; 7.8-8.2°E) and Steigen (67.7-67.9°N; 14.6-14.8°E), during the
128 breeding seasons of 2015 and 2016 (Figure 1). We sampled 35 nestlings both from Smøla
129 (2015: $n = 13$, 2016: $n = 22$) and Steigen (2015: $n = 14$, 2016: $n = 21$) during June-July of

130 these two years (see supplementary information (SI), Table S1 for details). Sex determination
131 was based upon morphometric measurements (Helander et al., 2007), while the age was
132 estimated from the tail feather length. The tail feather emerges at day 30 and grows with
133 (mean \pm SE) 4.95 ± 0.02 mm per day (Pers. comm. Torgeir Nygård). Wing length has
134 previously been used to estimate age in Swedish white-tailed eagle nestlings (Helander et al.,
135 2007) and in our study wing and tail feather length were strongly correlated ($r_{70} = 0.94$, $p <$
136 0.01). All nestlings were sampled for body feathers and blood as described in Løseth et al.
137 (2019). Body feathers were gently pulled from the dorsal region and stored in polyethylene
138 zipper bags (VWR, USA) at -20°C . A blood sample of 8 mL was collected in heparinised
139 vacutainers through brachial venepuncture. The blood samples were centrifuged at 860 g and
140 plasma was transferred into cryogenic tubes (Nalgene®, USA) and stored at -20°C . The
141 sampling was approved by the Norwegian Food Safety Authority (Mattilsynet; 2015/6432
142 and 2016/8709) and the handling of the birds were in accordance with the regulations of the
143 Norwegian Animal Welfare Act.

144 2.2. Stable isotope analyses

145 We analysed stable isotopes in the body feathers, which were still growing at the time of
146 sampling and thus connected to the blood circulation at the calami. The analysis for bulk
147 feather stable carbon (^{12}C and ^{13}C) and nitrogen isotopes (^{14}N and ^{15}N) was performed at the
148 MARE Centre of the University of Liège, Belgium. Clean stainless steel and glass tools were
149 used to remove the calami and for washing and cutting of the feathers. The tools were
150 thoroughly rinsed with acetone between individuals. Feathers were washed in Milli-Q water
151 as previously described in Løseth et al. (2019) to remove dust and particles from feathers
152 prior to analysis. A subsample of homogenised cleaned feather material (mean \pm SD: $1.55 \pm$
153 0.37 mg) was wrapped into a tin combustion cup and analysed for its elemental and isotopic
154 composition using a vario MICRO cube elemental analyser (Elementar Analysen systeme

155 GmbH, Hanau, Germany) coupled to an IsoPrime100 mass spectrometer (Isoprime, Cheadle,
156 United Kingdom). The reported stable carbon and nitrogen isotope values are expressed as δ
157 (‰) relative to the international reference standards Vienna PeeDee Belemnite and
158 atmospheric nitrogen, respectively. An internal reference material (i.e., glycine) was
159 measured for every tenth sample and revealed an imprecision (± 1 SD) of 0.23 and 0.16 ‰ for
160 $\delta^{13}\text{C}$ and $\delta^{15}\text{N}$, respectively.

161 2.3. Chemical analyses

162 The targeted compounds for the analyses were polychlorinated biphenyls (PCB; IUPAC
163 congeners 28, 49, 52, 74, 95, 99, 101, 105, 110, 118, 138, 149, 153, 156, 170, 171, 177, 180,
164 183, 187, 194, 206 and 209) and organochlorinated pesticides (OCPs;
165 dichlorodiphenyltrichloroethane (*p,p'*-DDT), *p,p'*-dichlorodiphenyldichloroethylene (*p,p'*-
166 DDE), three isomers of hexachlorocyclohexane (α -, β -, and γ -HCH), chlordanes (*oxy*-
167 chlordane (OxC), *cis*-nonachlor (CN) and *trans*-nonachlor (TN)) and hexachlorobenzene
168 (HCB)). The targeted legacy flame retardants were polybrominated diphenyl ether (PBDE)
169 congeners; BDE 28, 47, 99, 100, 153, 154 and 183. The targeted perfluoroalkyl substances
170 (PFASs) were perfluorobutanoic acid (PFBA), perfluoropentanoic acid (PFPeA),
171 perfluorohexanoic acid (PFHxA), perfluoroheptanoic acid (PFHpA), perfluorooctanoic acid
172 (PFOA), perfluorononanoic acid (PFNA), perfluorodecanoic acid (PFDcA),
173 perfluoroundecanoic acid (PFUnA), perfluorododecanoic acid (PFDoA), perfluorotridecanoic
174 acid (PFTrA), perfluorotetradecanoic acid (PFTeA), perfluorooctanesulfonamide (PFOSA),
175 perfluorobutane sulfonate (PFBA), perfluoropentane sulfonate (PFPS), perfluorohexane
176 sulfonate (PFHxS), perfluoroheptane sulfonate (PFHpS), linear and branched perfluorooctane
177 sulfonate (Lin-PFOS and Br-PFOS) and perfluorononane sulfonate (PFNS).

178 Procedures used for the extraction and quantification have been described in detail by Løseth
179 et al. (2019). In brief, PCBs, OCPs and PBDEs were extracted using *n*-
180 hexane:dichloromethane (DCM, 1:1, v:v) and fractionation was performed on Supelclean™
181 ENVI Florisil cartridges (500 mg, 3 mL, Supelco® Analytical). The compounds were eluted
182 with *n*-hexane:DCM and quantified according to Eulaers et al. (2011a). PFASs were
183 extracted with methanol using the Powley method (Powley et al., 2005) and quantified
184 according to Herzke et al. (2009). Internal standards and their recoveries are listed in SI
185 (Table S2 and S3) and ranged from 30 – 118 % for PCBs, 41 – 90 % for OCPs, 74 – 97 % for
186 PBDEs, and 59 – 101 % for PFASs. For every tenth plasma sample, a procedural blank was
187 analysed to control for background contamination. To control the performance of the
188 analytical method of the PCB, OCP and PBDE extraction, a human plasma sample from the
189 Arctic Monitoring and Assessment Programme interlaboratory exercise was analysed for
190 every 20th sample. For PFAS extractions, a commercially available human plasma sample
191 (NIST SRM 1957, USA) was analysed for every tenth sample. No background contamination
192 was encountered in the blanks for any of the analysed PFASs. For legacy POPs not detectable
193 in the blanks, the limits of quantification (LOQs) were set to ten times the signal-to-noise
194 ratio of sample runs or were calculated as three times the standard deviation of the procedural
195 blanks for each compound. For PFASs, the LOQs were calculated as three times the signal-
196 to-noise ratio of the procedural blanks for each compound. The LOQs for all compounds are
197 available in the SI (Tables S4-S6).

198 2.4. Statistical analyses

199 The statistical analyses were performed using R (v. 3.4.2, R Development Core Team, 2008).
200 The compounds that could be quantified in more than 50 % of the samples within each year
201 and location were 14 PCB congeners (CB 99, 101, 105, 118, 138, 153, 156, 170, 171, 177,
202 180, 183, 187 and 194), seven OCPs (OxC, TN, CN, *p,p'*-DDE, *p,p'*-DDT, HCB and β -

203 HCH), five PBDE congeners (BDE 47, 99, 100, 153 and 154) and eight PFASs (Br-PFOS,
204 Lin-PFOS, PFOA, PFNA, PFDcA, PFUnA, PFDoA and PFTriA) (Table 1 and Table S7).
205 Data below the limit of quantification (LOQ) were substituted with LOQ * detection
206 frequency (Voorspoels et al., 2002) for each compound. Profiles of the compounds included
207 in the statistical analyses are available in Figure S1. Due to the structure of the data, with two
208 to three chicks in some nests, only statistical tests from the *nlme*: Linear and nonlinear mixed
209 effect models package (Pinheiro et al., 2018) were applied and nest identity was always
210 included as a random variable to avoid pseudoreplication of nestlings within nests. Statistical
211 significance was assumed at $\alpha = 0.05$.

212 Due to collinearity between compounds within each contaminant group (Table S8 and S9),
213 compounds were summed (Σ) per group (Σ_{14} PCBs, Σ_7 OCPs, Σ_5 PBDEs and Σ_8 PFASs) for
214 statistical modelling. All variables were investigated for influential outliers, normality and
215 homoscedasticity (Zuur et al., 2010). Variables that were not normally distributed were \log_e
216 transformed to meet criteria of parametric statistics. To ensure normality of the residuals of
217 the model, two outliers were removed from the OCP modelling. These outliers were two
218 young individuals sampled in Steigen in 2015 (47.2 and 52.4 days old) which also had the
219 highest plasma concentrations of OCPs (46.3 and 52.2 ng/mL, respectively).

220 Age was included as an explanatory variable, instead of body mass or body condition due to
221 multicollinearity. It is important to note that each nestling was only sampled once and to
222 investigate the true variation with increasing age it is preferred to sample the same
223 individuals repeatedly. A detailed description of the calculation of body condition and
224 correlations between age, body mass and body condition can be found in the SI. Body mass,
225 size and age are all correlated when the nestlings are growing, but body mass may show large
226 variations between sexes and on an individual level due to different climates, habitats, diets

227 and parental experience. Age presents a more stable variable as it, on an individual level, can
228 only increase, regardless of sex and diet.

229 Correlations between $\log_e \Sigma$ contaminant groups, age, $\delta^{13}\text{C}$ and $\delta^{15}\text{N}$ were investigated using
230 Pearson correlation coefficient test. A strong correlation was detected between $\delta^{15}\text{N}$ and $\delta^{13}\text{C}$
231 ($r_{70} = 0.76$, $p < 0.01$, Figure S3), but both variables were included in the first model selection
232 as they represent trophic position and dietary source, respectively. To investigate temporal
233 and spatial variation of $\Sigma_{14}\text{PCBs}$, $\Sigma_7\text{OCPs}$, $\Sigma_5\text{PBDEs}$, $\Sigma_8\text{PFASs}$, age, $\delta^{13}\text{C}$ and $\delta^{15}\text{N}$, linear
234 mixed effect analyses of variance (Lme-Anovas) were applied with location, year and the
235 interaction between location and year as explanatory variables (Table S10). Tukey's honestly
236 significant difference (HSD) post hoc test was applied to investigate differences in age
237 between locations and years.

238 To investigate how age and the dietary proxies may contribute to the observed temporal and
239 spatial variation, we performed linear mixed effect models for each compound group. The
240 initial full model included location, year, the interaction between location and year, age, $\delta^{15}\text{N}$
241 and $\delta^{13}\text{C}$. The most parsimonious models were selected using Akaike's Information Criterion
242 for small sample sizes (AICc). Each model was analysed for variance inflation factors (VIF)
243 with a threshold of $\text{VIF} < 3$ to identify problems with collinearity among explanatory
244 variables (Zuur et al., 2009, 2010). The model selection showed that the effect of $\delta^{15}\text{N}$ was
245 only significant with the presence of $\delta^{13}\text{C}$ in the model, and VIF values for $\delta^{15}\text{N}$ were over 3
246 for some of the models. This may be due to the significant correlation detected between the
247 two stable isotopes. For the final model selection, we therefore chose to include only $\delta^{13}\text{C}$,
248 age, location, year and the interaction between location and year. Model selection was
249 performed on models fitted with maximum likelihood (ML), while parameters were estimated
250 using restricted maximum likelihood (REML). Models with $\Delta\text{AICc} < 2$ are discussed below.

251 In addition to AICc, marginal pseudo- R^2 (R_m^2 ; explaining the variation of the fixed factors)
252 and conditional pseudo- R^2 (R_c^2 ; explaining the variation of both fixed and random factors)
253 were extracted according to Nakagawa and Schielzeth (2013).

254 3. Results and discussion

255 3.1. Organohalogenated contaminants

256 The compound groups found with the highest median wet weight concentrations in plasma
257 were PFASs > PCBs > OCPs > PBDEs. Within each compound group, the compounds with
258 the highest concentrations were linear PFOS (3.86 – 31.85 ng/mL), CB 153 (0.21 – 26.27
259 ng/mL), *p,p'*-DDE (0.48 – 47.61 ng/mL) and BDE 47 (0.01 – 1.82 ng/mL), respectively
260 (Table S7). The concentrations of Σ_{14} PCBs, Σ_7 OCPs, Σ_5 PBDEs and Σ_8 PFASs (Table 1,
261 Figure S2A) were lower than or within the same range of those previously reported in plasma
262 from white-tailed eagle nestlings from Norway (Bustnes et al., 2013; Eulaers et al., 2011a,
263 2011b, 2013, 2014; Gómez-Ramírez et al., 2017).

264 3.2. Nestling age and dietary proxies

265 The age span of the nestlings varied significantly between locations and years, although the
266 nestlings were sampled within the same two calendar weeks each year (Table 1, Figure S2B).
267 In 2015, the nestlings from Smøla were on average 79 days old, which was 15 days older
268 than those from Steigen ($z = 3.5$, $p < 0.01$). The Smøla nestlings sampled in 2015 were also
269 13 days older than those sampled at Smøla and Steigen in 2016 ($z = 3.2 - 3.4$, $p < 0.01$, Table
270 S10). In 2016, there were no significant age differences between the nestlings sampled at
271 Smøla and Steigen. We also found significantly higher $\delta^{15}\text{N}$ and $\delta^{13}\text{C}$, as well as narrower
272 dietary niches, in nestlings from 2015 than in nestlings from 2016 ($F_{(1,44)} = 8.8$ and 4.9 , $p <$
273 0.01 , respectively, Figure S3, Table 1). The results also showed that the nestlings from

274 Steigen fed on a diet more enriched in ^{15}N than those from Smøla ($F_{(1,44)} = 15.7$, $p < 0.01$,
275 Figure S3), indicating that the Steigen nestlings may have been feeding on a higher trophic
276 position. The temporal variation found for both stable isotopes may indicate a slight change
277 in prey species between the two years at both locations. Within both years, some birds from
278 Smøla and Steigen had $\delta^{13}\text{C}$ values lower than -20‰ which indicates the influence of more
279 terrestrial prey in their diet (Fry, 2006). This was coherent with the observed prey remains
280 around their nests, which, besides from fish and seabirds, consisted of terrestrial species such
281 as greylag goose (*Anser anser*), hare (*Lepus timidus*) and hedgehogs (*Erinaceus europaeus*).
282 The interannual dietary changes reported here are not uncommon for opportunistic feeders
283 such as white-tailed eagles (Inger and Bearhop, 2008), as it can correspond to variations in
284 availability of prey species.

285 3.3. Model selection to best explain OHC variation

286 The results from the model selection confirmed age and diet as important predictors for the
287 temporal and spatial variation of legacy OHCs observed in the initial analyses (Table S10) as
288 they were included in all the most parsimonious models for PCBs, OCPs and PBDEs (Table
289 2, see Table S11 - S13 for all competing models). For PFASs on the other hand, only age was
290 selected as an important predictor for the observed temporal and spatial variation (Table S10)
291 as it was included in all the most parsimonious models for PFASs variation (Table 2, see
292 Table S14 for all competing models). It is important to note that these results are statistical
293 models which are estimating the OHC variation and in order to investigate the true OHCs
294 variation with increasing age, repeated sampling is necessary.

295 3.3.1 Legacy OHC variation

296 Contrary to our hypothesis, the models for $\Sigma_{14}\text{PCBs}$, $\Sigma_7\text{OCPs}$ and $\Sigma_5\text{PBDEs}$ indicated
297 significantly lower concentrations of legacy OHCs in older nestlings and in nestlings with a

328 diet more enriched in ^{13}C (i.e. more marine prey; Figure 2). Some of these models also
329 included location, year and the interaction between location and year, which contributed to a
330 better fit of the model. The results of the lme-Anova showed significant temporal and spatial
331 variation in PCB, OCP and PBDE levels (Table S10), however when we accounted for age
332 and diet in the model selection, the temporal and spatial variations for PCBs and PBDEs were
333 not significant anymore (Table 2). It was only for $\Sigma_7\text{OCPs}$ that the estimates indicated
334 significantly higher concentrations in nestlings from Steigen than those from Smøla ($p =$
335 0.01), as well as significantly higher concentration in nestlings from Steigen in 2015 than in
336 2016 ($p = 0.03$). In contrast to what was observed for $\Sigma_{14}\text{PCBs}$ and $\Sigma_5\text{PBDEs}$, the effect of
337 age was not statistically significant for $\Sigma_7\text{OCPs}$ ($\beta_1 = 0.012$, $p = 0.07$). However, it is
338 important to mention that for these models two of the youngest and most contaminated
339 individuals were excluded from the analyses to ensure normality of the residuals, and that the
340 inclusion of these outliers resulted in a significant effect of age on $\Sigma_7\text{OCPs}$ ($\beta_1 = 0.018$, $p =$
341 0.03). This should therefore be considered in the interpretation of the estimates of the $\Sigma_7\text{OCP}$
342 models.

343 3.3.1.1 Influence of age

344 The inverse relationship between plasma legacy OHC concentrations and age found in the
345 present study was in accordance with previous reports for CB 153 and p,p' -DDE in plasma of
346 white-tailed eagle nestlings (Bustnes et al., 2013), plasma levels of PCBs and PBDEs in great
347 tit (*Parus major*) nestlings (Dauwe et al., 2006) and liver concentrations of PCBs, p,p' -DDE
348 and HCB in European shag (*Phalacrocorax aristotelis*) nestlings (Jenssen et al., 2010;
349 Murvoll et al., 2006). In contrast, a previous study on white-tailed eagle nestlings did not find
350 decreased PCB or p,p' -DDE concentrations in plasma of older nestlings (Olsson et al., 2000),
351 neither did a study of PBDEs in plasma of bald eagle nestlings (Guo et al., 2018). The
352 nestlings from the present study were on average 69 days old (range: 44 – 87 days old), while

323 most of the nestlings from Olsson et al. (2000) were less than 57 days old (range: < 36 – 57
324 days old) and from Guo et al. (2018) were on average 46 days old (range: 28 – 56 days old).
325 Our significant effect of age may be due to the greater age span, larger sample size and
326 homogenous age classes in the present study, thus allowing more time for growth dilution or
327 changes in metabolic capability/excretion in older nestlings and a higher statistical
328 probability to detect such changes.

329 Even though nestlings are continuously exposed to OHCs through their diet, a study on
330 experimental feeding of great skua chicks (*Stercorarius skua*) found that their contaminant
331 load was more influenced by maternal than trophic transfer regardless of diet (Bourgeon et
332 al., 2013). A study of paired egg and plasma samples of bald eagled from the Great Lakes
333 between 2000 and 2012 found that egg concentrations of PBDEs were over 30 times higher
334 than the plasma concentrations of nestlings from the same nests (Guo et al., 2018). Nygård
335 and Polder (2012) also found very high concentrations of PCBs (mean: 2839 ng/g fresh
336 weight (fw)) and *p,p'*-DDE (mean: 950 ng/g fw) in white-tailed eagle eggs sampled in
337 Norway between 2005 and 2010. Although egg and plasma concentrations cannot be directly
338 compared, these reported concentrations were several folds higher than the plasma
339 concentrations found in the present study. As concentrations in plasma reflect internal
340 concentrations in the nestling, we propose that the decreasing legacy OHC concentrations
341 with increasing age may be due to growth dilution of maternally derived compounds
342 deposited with high concentrations in the eggs.

343 3.3.1.2 Influence of diet

344 Our results also indicated decreasing Σ_{14} PCBs, Σ_7 OCPs and Σ_5 PBDEs concentrations with
345 increasing $\delta^{13}\text{C}$, which corresponds with previous reports of decreases in CB 153, *p,p'*-DDE
346 and HCB in white-tailed eagle nestlings with diets more enriched in ^{13}C (Bustnes et al.,

347 2013). Bustnes et al. (2013) explained this relationship by the depleted ^{13}C levels found in
348 lipids compared to proteins (Post et al., 2007) and suggested that the diet of the more
349 contaminated nestlings may have contained more lipid-rich prey, such as gulls (*Laridae*),
350 which may also have contained higher concentrations of biomagnifying OHCs (Bustnes et al.,
351 2013). Surprisingly, the more contaminated nestlings from Smøla were feeding on a lower
352 trophic position (depleted in ^{15}N) and terrestrial prey remains were surrounding their nest
353 which were located more inland on the island. The contaminant concentrations in these
354 nestlings may therefore have been highly influenced by maternally derived OHCs (Bourgeon
355 et al., 2013). White-tailed eagles have been reported to change their diet in the winter
356 according to the availability of prey species (Willgohs, 1984). It is therefore possible that the
357 mothers of these nestlings have fed on a diet more enriched in lipids, containing higher
358 concentrations of OHCs, during the winter months and before egg laying. Such seasonal
359 dietary changes of the mothers may influence the concentrations of legacy OHCs in their
360 eggs and subsequently in their nestlings (Bourgeon et al., 2013). In contrast, stable isotopes
361 deposited in the keratin in nestling feathers originate mostly from their diet and not from
362 maternal transfer (Bearhop et al., 2002). Although we cannot be certain whether such a
363 dietary change has taken place, one should always keep in mind that the stable isotopes
364 analysed in feathers only reflect the diet in the period during which they were grown
365 (Bearhop et al., 2002).

366 A study on bald eagle nestlings also found that $\delta^{13}\text{C}$ was generally a better predictor of legacy
367 OHC concentrations than $\delta^{15}\text{N}$ in eagles from marine environments, even when the two stable
368 isotope ratios were correlated (Elliott et al., 2015). This was confirmed by the results in the
369 current study as the final model selection did not include $\delta^{15}\text{N}$ and no significant correlations
370 were found between $\delta^{15}\text{N}$ and the OHC groups. However, significant positive correlations
371 between $\delta^{15}\text{N}$ or trophic level and several legacy POPs have been found in previous studies

372 on both white-tailed eagle (Bustnes et al., 2013; Eulaers et al., 2013, 2014) and bald eagle
373 nestlings (*Haliaeetus leucocephalus*; Elliott et al., 2015).

374 3.3.2. PFAS variation

375 Contrary to the legacy OHCs models, the models for PFASs indicated no significant effect of
376 $\delta^{13}\text{C}$ on PFAS concentrations in plasma and the most parsimonious model included age,
377 location and year (Table 2, Figure 3). These results were not unexpected as PFASs have
378 different physicochemical properties than legacy OHCs and may therefore have different
379 exposure routes and toxicokinetics (Lau et al., 2007).

380 3.3.2.1 Influence of age

381 Interestingly, we found opposite age-related effects for PFASs than for PCBs, OCPs and
382 PBDEs, confirming our initial hypothesis of increasing plasma concentrations with increasing
383 age. A similar increase with age has also been reported earlier for PFOS in white-tailed eagle
384 nestlings (Bustnes et al., 2013) and for PFNA and PFUnA in bald eagle nestlings (Route et
385 al., 2014). The PFAS concentrations in the current study were also similar to the
386 concentrations found in white-tailed eagle eggs from Norway in 2005 – 2010 (mean: 55.3
387 ng/g fw; Nygård and Polder, 2012), which suggest that maternal transfer may be of less
388 importance for PFAS exposure than for the legacy OHCs. The increasing PFAS
389 concentrations with age are therefore more likely originating from dietary sources, than from
390 maternal transfer, as maternally deposited concentrations are diluted by growth regardless of
391 the physicochemical properties of the compounds (Bustnes et al., 2013).

392 3.3.2.2 Spatial variation

393 The model estimates also indicated significantly higher PFAS concentrations in nestlings
394 from Steigen than in those from Smøla (Table 2, $p < 0.01$). At the same time, significantly

395 higher $\delta^{15}\text{N}$ were detected in nestlings from Steigen than nestlings from Smøla as well as
396 significant correlations between PFAS concentrations and $\delta^{13}\text{C}$ ($r_{70} = 0.25$, $p = 0.03$) and
397 $\delta^{15}\text{N}$ ($r_{70} = 0.44$, $p < 0.01$). Thus, we cannot exclude trophic position as an important factor
398 influencing this PFAS variation. Nevertheless, the absence of stable isotopes in the most
399 parsimonious PFAS models corresponds with previous reports in plasma from Norwegian
400 white-tailed eagle nestlings (Bustnes et al., 2013; Gómez-Ramírez et al., 2017) and several
401 seabirds (Gebbinck et al., 2011; Haukås et al., 2007; Leat et al., 2013; Miller et al., 2015;
402 Vicente et al., 2015).

403 *3.3.2.3 Temporal variation*

404 The model also indicated significantly higher PFAS concentrations in nestlings sampled in
405 2015 than in 2016, at both locations (Table 2, $p < 0.01$). This interannual variation
406 corresponds with a previous study on white-tailed eagle nestlings from Troms and
407 Vesterålen, Norway in 2011 and 2012 (Sletten et al., 2016). The authors of that study
408 suggested dietary differences as the main reason for that variation (Sletten et al., 2016),
409 which corresponds with the present study as we also detected significant differences in stable
410 isotopes between years. Interestingly, the difference between 2015 and 2016 in PFAS plasma
411 concentrations in the present study also corresponds with reports on PFASs in air, where
412 higher concentrations of several PFASs were found at three monitoring stations in Norway in
413 2015 compared to 2016 (Bohlin-Nizzetto et al., 2017; Bohlin-Nizzetto and Aas, 2016). Thus,
414 yearly differences in long range transport of PFASs and its precursors may play a role, as
415 they can be subsequently taken up into the food web (Houde et al., 2011) and their top
416 predators (Bustnes et al., 2015). To our knowledge, there are no significant PFAS sources at
417 the two locations that may influence PFASs concentrations in the white-tailed eagle nestlings.
418 However, due to the significantly higher stable isotope values in nestlings from 2015 and
419 correlation between $\delta^{15}\text{N}$ values and PFAS concentrations, we suggest a combination of

420 PFAS exposure from long range transport and dietary sources as important factors explaining
421 this temporal variation.

422 4. Conclusions

423 In the present study, we report age as one of the most important predictors for spatial and
424 temporal variation of OHCs in plasma from white-tailed eagle nestlings from Smøla and
425 Steigen, Norway. It is important to note that the nestlings in the present study were only
426 sampled once, and that the models were based on results from nestlings ranging from 44 to
427 87 days old. Our results indicated lower plasma concentrations of PCBs, PBDEs and OCPs in
428 older nestlings, while the concentrations of PFASs were higher in the older nestlings. The
429 variations in PCBs, OCPs and PBDEs were also significantly explained by the dietary carbon
430 source ($\delta^{13}\text{C}$), indicating that nestlings feeding on a diet with more marine prey had lower
431 plasma concentrations of these compounds. The stable isotope ratio of nitrogen ($\delta^{15}\text{N}$) was of
432 less importance in the present study, however it indicated that nestlings from Steigen were
433 feeding at a higher trophic position than those from Smøla. We also found higher stable
434 isotope ratios in nestlings sampled in 2015 compared to 2016 which may suggest dietary
435 differences. Overall, our results indicate a need to take age into consideration when
436 investigating OHC concentrations in bird of prey nestlings, regardless of the sample matrix
437 (as strong correlations were found between concentrations of PCBs, OCPs and PBDEs in
438 feathers, plasma and preen oil; see Løseth et al., 2019). Our results also indicate that diet may
439 contribute to variations in plasma OHC concentrations, especially for PCBs, OCPs and
440 PBDEs in opportunistic birds such as the white-tailed eagle.

441 5. Acknowledgements

442 The authors acknowledge the Norwegian Research Council and NTNU for funding Mari E.
443 Løseth, Nathalie Briels, Veerle L.B. Jaspers and the NewRaptor project (# 230465). Giulia

444 Poma and Govindan Malarvannan acknowledge funding from the University of Antwerp for
445 their post-doc fellowships. Trond V. Johnsen, Paula Marcinekova, Jørgen Flo, Courtney
446 Waugh, Espen L. Dahl, Johannes Schrøder and Aasmund Gylseth are acknowledged for their
447 assistance during sample collection. We thank Grethe S. Eggen, Lene N. Torgersen from
448 NTNU and Linda Hanssen from NILU for assisting with the chemical analyses. Additional
449 funding for fieldwork in Steigen was provided by the Hazardous Substances Flagship (the
450 Raptor project) at the Fram Center in Tromsø.

451 6. References

- 452 Bearhop, S., Waldron, S., Votier, S.C., Furness, R.W., 2002. Factors That Influence
453 Assimilation Rates and Fractionation of Nitrogen and Carbon Stable Isotopes in Avian
454 Blood and Feathers. *Physiol. Biochem. Zool.* 75, 451–458. doi:10.1086/342800
- 455 Bohlin-Nizzetto, P., Aas, W., 2016. Monitoring of environmental contaminants in air and
456 precipitation, annual report 2015. Norwegian Environmental Agency. ISBN: 978-82-
457 425-2841-4
- 458 Bohlin-Nizzetto, P., Aas, W., Warner, N., 2017. Monitoring of environmental contaminants
459 in air and precipitation, annual report 2016. Norwegian Environmental Agency. ISBN:
460 978-82-425-2888-9
- 461 Borgå, K., Fisk, A.T., Hoekstra, P.E., Muir, D.C.G., 2004. Biological and chemical factors of
462 importance in the bioaccumulation and trophic transfer of persistent organochlorine
463 contaminants in Arctic marine food webs. *Environ. Toxicol. Chem.* 23, 2367–2385.
464 doi:10.1897/03-518
- 465 Borgå, K., Kidd, K.A., Muir, D.C.G., Berglund, O., Conder, J.M., Gobas, F.A.P.C.,
466 Kucklick, J., Malm, O., Powell, D.E., 2012. Trophic magnification factors:

467 Considerations of ecology, ecosystems, and study design. *Integr. Environ. Assess.*
468 *Manag.* 8, 64–84. doi:10.1002/ieam.244

469 Bourgeon, S., Leat, E.K.H., Furness, R.W., Borgå, K., Hanssen, S.A., Bustnes, J.O., 2013.
470 Dietary versus maternal sources of organochlorines in top predator seabird chicks: An
471 experimental approach. *Environ. Sci. Technol.* 47, 5963–5970. doi:10.1021/es400442q

472 Bustnes, J.O., Bårdsen, B.J., Herzke, D., Johnsen, T. V, Eulaers, I., Ballesteros, M., Hanssen,
473 S. a, Covaci, A., Jaspers, V.L.B., Eens, M., Sonne, C., Halley, D., Moum, T., Nøst, T.H.,
474 Erikstad, K.E., Ims, R.A., 2013. Plasma concentrations of organohalogenated pollutants
475 in predatory bird nestlings: associations to growth rate and dietary tracers. *Environ.*
476 *Toxicol. Chem.* 32, 2520–2527. doi:10.1002/etc.2329

477 Bustnes, J.O., Bangjord, G., Ahrens, L., Herzke, D., Yoccoz, N.G., 2015. Perfluoroalkyl
478 substance (PFAS) concentrations in a terrestrial raptor: Relationships to environmental
479 conditions and individual traits. *Environ. Toxicol. Chem.* 34, 184–191.
480 doi:10.1002/etc.2782

481 Cassone, C.G., Vongphachan, V., Chiu, S., Williams, K.L., Letcher, R.J., Pelletier, E.,
482 Crump, D., Kennedy, S.W., 2012. In ovo effects of perfluorohexane sulfonate and
483 perfluorohexanoate on pipping success, development, mRNA expression, and thyroid
484 hormone levels in chicken embryos. *Toxicol. Sci.* 127, 216–224.
485 doi:10.1093/toxsci/kfs072

486 Dauwe, T., Jaspers, V.L.B., Covaci, A., Eens, M., 2006. Accumulation of organochlorines
487 and brominated flame retardants in the eggs and nestlings of great tits, *Parus major*.
488 *Environ. Sci. Technol.* 40, 5297–5303. doi:10.1021/es060747a

489 Elliott, J.E., Brogan, J., Lee, S.L., Drouillard, K.G., Elliott, K.H., 2015. PBDEs and other

490 POPs in urban birds of prey partly explained by trophic level and carbon source. *Sci.*
491 *Total Environ.* 524–525, 157–165. doi:10.1016/j.scitotenv.2015.04.008

492 Eulaers, I., Covaci, A., Hofman, J., Nygård, T., Halley, D.J., Pinxten, R., Eens, M., Jaspers,
493 V.L.B., 2011a. A comparison of non-destructive sampling strategies to assess the
494 exposure of white-tailed eagle nestlings (*Haliaeetus albicilla*) to persistent organic
495 pollutants. *Sci. Total Environ.* 410–411, 258–265. doi:10.1016/j.scitotenv.2011.09.070

496 Eulaers, I., Covaci, A., Herzke, D., Eens, M., Sonne, C., Moum, T., Schnug, L., Hanssen,
497 S.A., Johnsen, T.V., Bustnes, J.O., Jaspers, V.L.B., 2011b. A first evaluation of the
498 usefulness of feathers of nestling predatory birds for non-destructive biomonitoring of
499 persistent organic pollutants. *Environ. Int.* 37, 622–30. doi:10.1016/j.envint.2010.12.007

500 Eulaers, I., Jaspers, V.L.B., Bustnes, J.O., Covaci, A., Johnsen, T. V., Halley, D.J., Moum,
501 T., Ims, R.A., Hanssen, S.A., Erikstad, K.E., Herzke, D., Sonne, C., Ballesteros, M.,
502 Pinxten, R., Eens, M., 2013. Ecological and spatial factors drive intra- and interspecific
503 variation in exposure of subarctic predatory bird nestlings to persistent organic
504 pollutants. *Environ. Int.* 57–58, 25–33. doi:10.1016/j.envint.2013.03.009

505 Eulaers, I., Jaspers, V.L.B., Halley, D.J., Lepoint, G., Nygård, T., Pinxten, R., Covaci, A.,
506 Eens, M., 2014. Brominated and phosphorus flame retardants in White-tailed Eagle
507 *Haliaeetus albicilla* nestlings: bioaccumulation and associations with dietary proxies
508 ($\delta^{13}\text{C}$, $\delta^{15}\text{N}$ and $\delta^{34}\text{S}$). *Sci. Total Environ.* 478, 48–57.
509 doi:10.1016/j.scitotenv.2014.01.051

510 Faxneld, S., Berger, U., Helander, B., Danielsson, S., Miller, A., Nyberg, E., Persson, J.-O.,
511 Bignert, A., 2016. Temporal Trends and Geographical Differences of Perfluoroalkyl
512 Acids in Baltic Sea Herring and White-Tailed Sea Eagle Eggs in Sweden. *Environ. Sci.*

513 Technol. 50, 13070–13079. doi:10.1021/acs.est.6b03230

514 Fry, B., 2006. Stable isotope ecology, Stable Isotope Ecology. Springer Science, USA.
515 doi:10.1007-0-387-33745-8

516 Gebbink, W.A., Letcher, R.J., Hebert, C.E., Chip Weseloh, D. V., 2011. Twenty years of
517 temporal change in perfluoroalkyl sulfonate and carboxylate contaminants in herring
518 gull eggs from the Laurentian Great Lakes. J. Environ. Monit. 13, 3365–3372.
519 doi:10.1039/c1em10663e

520 Gómez-Ramírez, P., Bustnes, J.O., Eulaers, I., Herzke, D., Johnsen, T.V., Lepoint, G., Pérez-
521 García, J.M., García-Fernández, A.J., Jaspers, V.L.B., 2017. Per- and polyfluoroalkyl
522 substances in plasma and feathers of nestling birds of prey from northern Norway.
523 Environ. Res. 158, 277–285. doi:10.1016/j.envres.2017.06.019

524 Guo, J., Simon, K., Romanak, K., Bowerman, W., Venier, M., 2018. Accumulation of flame
525 retardants in paired eggs and plasma of bald eagles. Environ. Pollut. 237, 499–507.
526 doi:10.1016/j.envpol.2018.02.056

527 Haukås, M., Berger, U., Hop, H., Gulliksen, B., Gabrielsen, G.W., 2007. Bioaccumulation of
528 per- and polyfluorinated alkyl substances (PFAS) in selected species from the Barents
529 Sea food web. Environ. Pollut. 148, 360–371. doi:10.1016/j.envpol.2006.09.021

530 Helander, B., Bignert, A., Asplund, L., 2008. Using raptors as environmental sentinels:
531 monitoring the white-tailed sea eagle *Haliaeetus albicilla* in Sweden. Ambio A J. Hum.
532 Environ. 37, 425–431. doi:10.1579/0044-7447(2008)37

533 Helander, B., Hailer, F., Vilà, C., 2007. Morphological and genetic sex identification of
534 white-tailed eagle *Haliaeetus albicilla* nestlings. J. Ornithol. 148, 435–442.
535 doi:10.1007/s10336-007-0156-y

536 Helgason, L.B., Barrett, R., Lie, E., Polder, A., Skaare, J.U., Gabrielsen, G.W., 2008. Levels
537 and temporal trends (1983-2003) of persistent organic pollutants (POPs) and mercury
538 (Hg) in seabird eggs from Northern Norway. *Environ. Pollut.* 155, 190–198.
539 doi:10.1016/j.envpol.2007.10.022

540 Herzke, D., Nygård, T., Berger, U., Huber, S., Rørv, N., 2009. Perfluorinated and other
541 persistent halogenated organic compounds in European shag (*Phalacrocorax aristotelis*)
542 and common eider (*Somateria mollissima*) from Norway: a suburban to remote pollutant
543 gradient. *Sci. Total Environ.* 408, 340–348. doi:10.1016/j.scitotenv.2009.08.048

544 Houde, M., De Silva, A.O., Muir, D.C.G., Letcher, R.J., Canada, E., Saint-laurent, C., Street,
545 M., 2011. Monitoring of Perfluorinated Compounds in Aquatic Biota: An Updated
546 Review. *Environ. Sci. Technol.* 45, 7962–7973. doi: 10.1021/es104326w

547 Hung, H., Katsoyiannis, A.A., Brorström-Lundén, E., Olafsdottir, K., Aas, W., Breivik, K.,
548 Bohlin-Nizzetto, P., Sigurdsson, A., Hakola, H., Bossi, R., Skov, H., Sverko, E., Barresi,
549 E., Fellin, P., Wilson, S., 2016. Temporal trends of Persistent Organic Pollutants (POPs)
550 in arctic air: 20 years of monitoring under the Arctic Monitoring and Assessment
551 Programme (AMAP). *Environ. Pollut.* 217, 52–61. doi:10.1016/j.envpol.2016.01.079

552 Inger, R., Bearhop, S., 2008. Applications of stable isotope analyses to avian ecology. *Ibis*
553 (Lond. 1859). 447–461. doi:10.1111/j.1474-919X.2008.00839.x

554 Jenssen, B.M., Aarnes, J.B., Murvoll, K.M., Herzke, D., Nygård, T., 2010. Fluctuating wing
555 asymmetry and hepatic concentrations of persistent organic pollutants are associated in
556 European shag (*Phalacrocorax aristotelis*) chicks. *Sci. Total Environ.* 408, 578–585.
557 doi:10.1016/j.scitotenv.2009.10.036

558 Kelly, J.F., 2000. Stable isotopes of carbon and nitrogen in the study of avian and mammalian

559 trophic ecology. Can. J. Zool. 78, 1–27. doi:10.1139/z99-165

560 Koivusaari, J., Nuuja, I., Palokangas, R., Hattula, M.-L., 1976. Chlorinated Hydrocarbons
561 and Total Mercury in the Prey of the White-tailed Eagle (*Haliaeetus albicilla* L .) in the
562 Quarken Straits of the Gulf of Bothnia , Finland. Bull. Environ. Contam. Toxicol. 15,
563 235–241.

564 Lau, C., Anitole, K., Hodes, C., Lai, D., Pfahles-Hutchens, A., Seed, J., 2007. Perfluoroalkyl
565 acids: a review of monitoring and toxicological findings. Toxicol. Sci. 99, 366–94.
566 doi:10.1093/toxsci/kfm128

567 Leat, E.H.K., Bourgeon, S., Borgå, K., Strøm, H., Hanssen, S.A., Gabrielsen, G.W., Petersen,
568 Æ., Olafsdottir, K., Magnusdottir, E., Fisk, A.T., Ellis, S., Bustnes, J.O., Furness, R.W.,
569 2011. Effects of environmental exposure and diet on levels of persistent organic
570 pollutants (POPs) in eggs of a top predator in the North Atlantic in 1980 and 2008.
571 Environ. Pollut. 159, 1222–1228. doi:10.1016/j.envpol.2011.01.036

572 Leat, E.H.K., Bourgeon, S., Eze, J.I., Muir, D.C.G., Williamson, M., Bustnes, J.O., Furness,
573 R.W., Borgå, K., 2013. Perfluoroalkyl substances in eggs and plasma of an avian top
574 predator, great skua (*Stercorarius skua*), in the north Atlantic. Environ. Toxicol. Chem.
575 32, 569–576. doi:10.1002/etc.2101

576 Løseth, M.E., Briels, N., Flo, J., Malarvannan, G., Poma, G., Covaci, A., Herzke, D., Nygård,
577 T., Bustnes, J.O., Jenssen, B.M., Jaspers, V.L.B., 2019. White-tailed eagle (*Haliaeetus*
578 *albicilla*) feathers from Norway are suitable for monitoring of legacy, but not emerging
579 contaminants. Sci. Total Environ. 647, 525–533. doi:10.1016/j.scitotenv.2018.07.333

580 Mackay, D., Shiu, W.Y., Ma, K., Lee, S.C., 2006. Halogenated Hydrocarbons, Second edi.
581 ed, Handbook of Physical-Chemical Properties and Environmental Fate for Organic

582 Chemicals, Second Edition. CRC Press, Taylor & Francis Group.

583 Miller, A., Elliott, J.E., Elliott, K.H., Lee, S., Cyr, F., 2015. Temporal trends of
584 perfluoroalkyl substances (PFAS) in eggs of coastal and offshore birds: Increasing
585 PFAS levels associated with offshore bird species breeding on the Pacific coast of
586 Canada and wintering near Asia. *Environ. Toxicol. Chem.* 34, 1799–1808.
587 doi:10.1002/etc.2992

588 Muir, D.C.G., de Wit, C.A., 2010. Trends of legacy and new persistent organic pollutants in
589 the circumpolar arctic: Overview, conclusions, and recommendations. *Sci. Total
590 Environ.* 408, 3044–3051. doi:10.1016/j.scitotenv.2009.11.032

591 Murvoll, K.M., Skaare, J.U., Anderssen, E., Jenssen, B.M., 2006. Exposure and effects of
592 persistent organic pollutants in European shag (*Phalacrocorax aristotelis*) hatchlings
593 from the coast of Norway. *Environ. Toxicol. Chem.* 25, 190–198. doi:10.1897/04-
594 333R.1

595 Nakagawa, S., Schielzeth, H., 2013. A general and simple method for obtaining R² from
596 generalized linear mixed-effects models. *Methods Ecol. Evol.* 4, 133–142.
597 doi:10.1111/j.2041-210x.2012.00261.x

598 Nordlöf, U., Helander, B., Bignert, A., Asplund, L., 2010. Levels of brominated flame
599 retardants and methoxylated polybrominated diphenyl ethers in eggs of white-tailed sea
600 eagles breeding in different regions of Sweden. *Sci. Total Environ.* 409, 238–246.
601 doi:10.1016/j.scitotenv.2010.09.042

602 Nøst, T.H., Helgason, L.B., Harju, M., Heimstad, E.S., Gabrielsen, G.W., Jenssen, B.M.,
603 2012. Halogenated organic contaminants and their correlations with circulating thyroid
604 hormones in developing Arctic seabirds. *Sci. Total Environ.* 414, 248–56.

605 doi:10.1016/j.scitotenv.2011.11.051

606 Nygård, T., Polder, A., 2012. Miljøgifter i rovfuglegg i Norge. Tilstand og tidstrender,
607 Norwegian Institute for Nature research (NINA), report 834. ISBN: 978-82-426-2429-1

608 Olsson, A., Ceder, K., Bergman, Å., Helander, B., 2000. Nestling blood of the white-tailed
609 sea eagle (*Haliaeetus albicilla*) as an indicator of territorial exposure to organohalogen
610 compounds - An evaluation. Environ. Sci. Technol. 34, 2733–2740.
611 doi:10.1021/es991426k

612 Pinheiro, J., Bates, D., DebRoy, S., Sarkar, D., Heisterkamp, S., Van Willigen, B., 2018.

613 nlme: Linear and Nonlinear Mixed Effects Models. R Package version 3.1-131.

614 Post, D.M., Layman, C.A., Arrington, D.A., Takimoto, G., Quattrochi, J., Montaña, C.G.,
615 2007. Getting to the fat of the matter: Models, methods and assumptions for dealing with
616 lipids in stable isotope analyses. Oecologia 152, 179–189. doi:10.1007/s00442-006-
617 0630-x

618 Powley, C.R., George, S.W., Ryan, T.W., Buck, R.C., 2005. Matrix effect-free analytical
619 methods for determination of perfluorinated carboxylic acids in environmental matrixes.
620 Anal. Chem. 77, 6353–6358. doi:10.1021/ac0508090

621 R Development Core Team, 2008. R: A language and environment for statistical computing.

622 Route, W.T., Key, R.L., Russell, R.E., Lindstrom, A.B., Strynar, M.J., 2014. Spatial and
623 temporal patterns in concentrations of perfluorinated compounds in bald eagle nestlings
624 in the upper Midwestern United States. Environ. Sci. Technol. 48, 6653–6660.
625 doi:10.1021/es501055d

626 Sletten, S., Bourgeon, S., Bårdsen, B.-J., Herzke, D., Criscuolo, F., Massemin, S., Zahn, S.,

627 Johnsen, T.V., Bustnes, J.O., 2016. Organohalogenated contaminants in white-tailed
628 eagle (*Haliaeetus albicilla*) nestlings: An assessment of relationships to immunoglobulin
629 levels, telomeres and oxidative stress. *Sci. Total Environ.* 539, 337–349.
630 doi:10.1016/j.scitotenv.2015.08.123

631 UNEP (United Nations Environmental Programme), 2009. The Stockholm Convention on
632 Persistent Organic Pollutants. United Nations, adoption of amendments to Annexes A, B
633 and C. Stock. Conv. URL:
634 <http://chm.pops.int/Convention/ConventionText/tabid/2232/Default.aspx>

635 Vicente, J., Sanpera, C., García-Tarrasón, M., Pérez, A., Lacorte, S., 2015. Perfluoroalkyl and
636 polyfluoroalkyl substances in entire clutches of Audouin's gulls from the ebro delta.
637 *Chemosphere* 119, S62–S68. doi:10.1016/j.chemosphere.2014.04.041

638 Voorspoels, S., Covaci, A., Maervoet, J., Schepens, P., 2002. Relationship between age and
639 levels of organochlorine contaminants in human serum of a Belgian population. *Bull.*
640 *Environ. Contam. Toxicol.* 69, 22–29. doi:10.1007/s00128-002-0004-y

641 Wang, Z., Cousins, I.T., Scheringer, M., Buck, R.C., Hungerbühler, K., 2014. Global
642 emission inventories for C4-C14perfluoroalkyl carboxylic acid (PFCA) homologues
643 from 1951 to 2030, Part I: Production and emissions from quantifiable sources. *Environ.*
644 *Int.* 70, 62–75. doi:10.1016/j.envint.2014.04.013

645 Wierda, M.R., Leith, K.F., Roe, A.S., Grubb, T.G., Sikarskie, J.G., Best, D.A., Pittman, H.T.,
646 Fuentes, L., Simon, K.L., Bowerman, W., 2016. Using bald eagles to track spatial
647 (1999–2008) and temporal (1987–1992, 1999–2003, and 2004–2008) trends of
648 contaminants in Michigan's aquatic ecosystems. *Environ. Toxicol. Chem.* 35, 1995–
649 2002. doi:10.1002/etc.3523

650 Willgohs, J.F., 1984. Havørn i Norge: Næring, forplantningsøkologi, konkurrenter og fiender.
651 Direktoratet for vilt og ferskvannsfisk, Trondheim. ISSN:032-5008

652 Zuur, A.F., Ieno, E.N., Elphick, C.S., 2010. A protocol for data exploration to avoid common
653 statistical problems. *Methods Ecol. Evol.* 1, 3–14. doi:10.1111/j.2041-
654 210X.2009.00001.x

655 Zuur, A.F., Ieno, E.N., Walker, N.J., Saveliev, A.A., Smith, G.M., 2009. *Mixed Effects*
656 *Models and Extensions in Ecology with R*, Springer.
657 doi:10.1017/CBO9781107415324.00

658

659 List of figures

660 **Figure 1:** Map of Norway (A) showing the two white-tailed eagle populations in the study, Smøla (B) and
661 Steigen (C). Nests sampled in 2015 are indicated by circles and 2016 by triangles, at both locations.

662 **Figure 1:** The most parsimonious model for variation of Σ_{14} PCBs concentrations (\log_e ng/mL) in plasma of
663 white-tailed eagle nestlings from Smøla and Steigen. The model estimates a significant decrease in Σ_{14} PCB
664 levels with increasing age and increasing $\delta^{13}\text{C}$ values in the nestlings' feathers. The model also included
665 location, however the effect was not statistically significant ($p = 0.08$) and therefore not presented here.

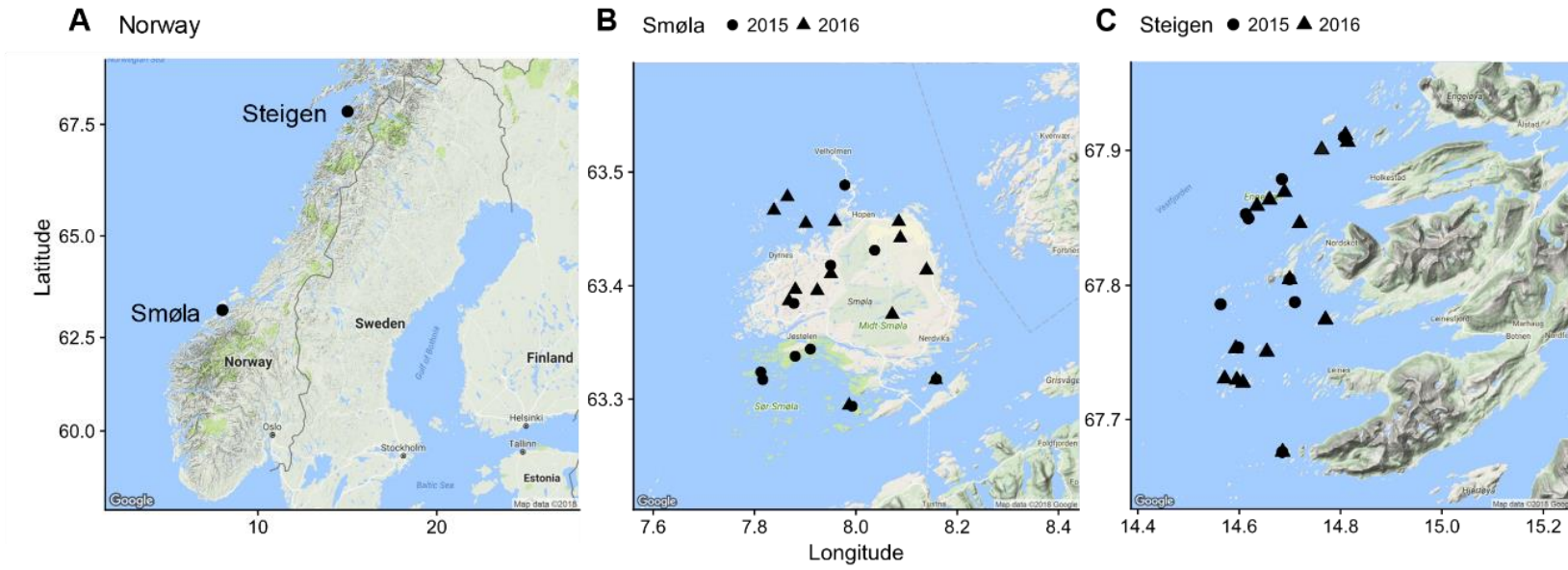
666 **Figure 2:** The most parsimonious model for variation of Σ_8 PFASs concentration (\log_e ng/mL) in plasma of
667 white-tailed eagle nestlings from Smøla and Steigen, Norway. The model estimates an increase in Σ_8 PFAS
668 levels with increasing age and shows significant differences between years and locations.

669

670

671 **Figure 1**

672



673

Figure 2

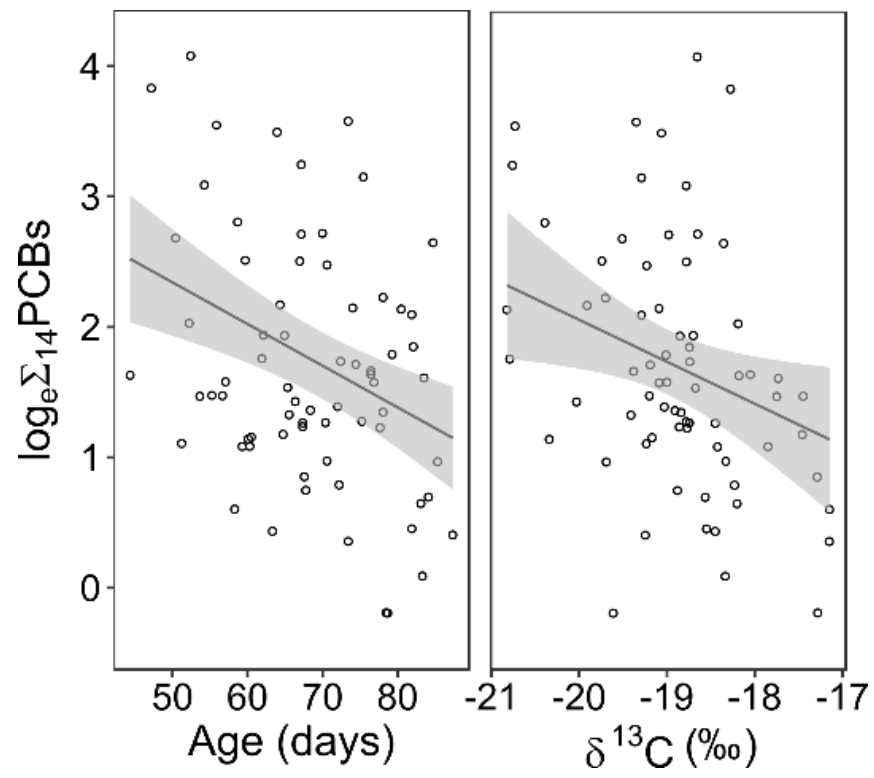


Figure 3

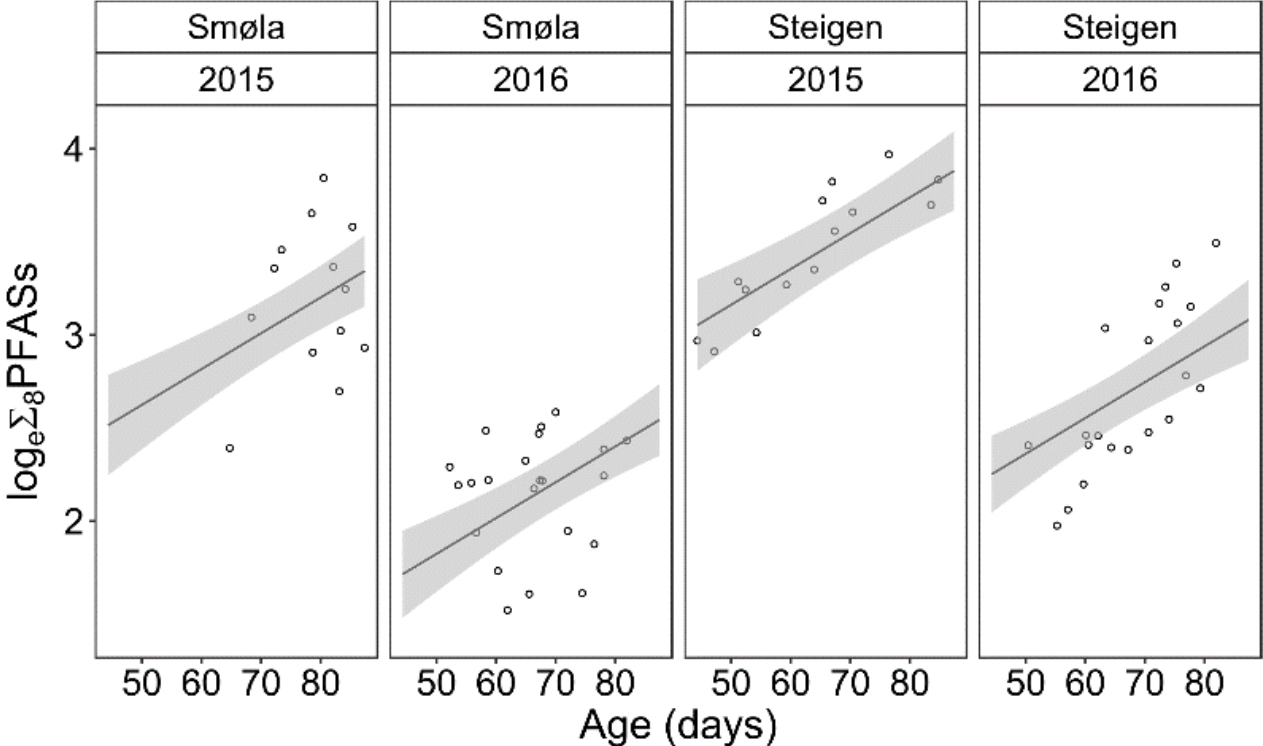


Table 1: Median, min and max values of stable isotopes from body feathers, age and sum of PCBs, OCPs, PBDEs and PFASs detected in plasma of white-tailed eagle nestlings sampled in Smøla and Steigen (Norway) in 2015 and 2016. A full list of concentration data for the individual compounds can be found in Løseth et al. (2019).

Smøla							Steigen						
2015 <i>n</i> = 13			2016 <i>n</i> = 22				2015 <i>n</i> = 14			2016 <i>n</i> = 21			
	unit	median	min	max	median	Min	max	median	min	max	median	min	max
$\delta^{13}\text{C}$	‰	-18.56	-20.82	-17.15	-19.02	-20.79	-17.15	-18.66	-19.24	-17.73	-19.11	-20.34	-18.33
$\delta^{15}\text{N}$	‰	+13.82	+12.45	+15.07	+13.39	+11.54	+15.28	+14.54	+13.89	+15.17	+13.96	+13.43	+14.73
Age	days	80.51	64.75	87.37	66.77	52.22	81.92	64.65	44.34	84.75	70.61	50.40	81.92
$\Sigma_{14}\text{PCBs}^{\text{a}}$	ng/mL	2.00	0.82	8.47	4.86	1.86	34.52	5.12	2.95	59.05	5.79	1.58	35.92
$\Sigma_7\text{OCPs}^{\text{b}}$	ng/mL	2.01	0.89	6.28	2.75	1.05	15.33	4.75	2.80	52.19	5.79	1.31	12.96
$\Sigma_5\text{PBDEs}^{\text{c}}$	ng/mL	0.10	0.06	0.46	0.16	0.05	1.51	0.34	0.10	2.64	0.23	0.03	0.73
$\Sigma_8\text{PFASs}^{\text{d}}$	ng/mL	25.69	10.29	46.65	9.18	4.58	13.26	31.80	18.36	52.94	12.76	7.21	32.90

^a $\Sigma_{14}\text{PCBs}$: CB 99, 101, 105, 118, 138, 153, 156, 170, 171, 177, 180, 183, 187 and 194

^b $\Sigma_7\text{OCPs}$: OxC, TN, CN, *p,p'*-DDE, *p,p'*-DDT, HCB and β -HCH

^c $\Sigma_5\text{PBDEs}$: BDE 47, 99, 100, 153 and 154

^d $\Sigma_8\text{PFASs}$: Br-PFOS, Lin-PFOS, PFOA, PFNA, PFDcA, PFUnA, PFDoA and PFTriA

- 1 **Table 2:** Model estimates from the most parsimonious models ($\Delta\text{AICc} < 2$) explaining the variation of $\Sigma_{14}\text{PCBs}$, $\Sigma_7\text{OCPs}$, $\Sigma_5\text{PBDEs}$ and $\Sigma_8\text{PFASs}$ in plasma of white-tailed
2 eagle nestlings ($n = 70$) from Smøla and Steigen. The table includes the model intercept (β_0), model estimates (β_x), significance values (p), and marginal pseudo- R^2 (R_m^2) and
3 conditional pseudo- R^2 (R_c^2). The year variable (Yr) represents 2016 and location variable (Loc) represents Steigen. Beta estimates follow the order of the factors in the
4 models. Statistical significance ($\alpha = 0.05$) is marked with *.

Compound group	Explanatory variables	β_0	β_1	β_2	β_3	β_4	β_5	<i>p-values</i>	ΔAICc	R_m^2	R_c^2
$\Sigma_{14}\text{PCBs}$	~ age + $\delta^{13}\text{C}$ + Loc	-3.07	-0.03	-0.36	0.43			<0.01*; 0.01*; 0.08	0.00	0.28	0.89
	~ age + $\delta^{13}\text{C}$	-2.61	-0.03	-0.35				<0.01*; 0.01*	0.81	0.22	0.89
	~ age + $\delta^{13}\text{C}$ + Loc + Yr + Loc:Yr	-3.66	-0.03	-0.35	1.03	0.57	-0.95	0.01*; 0.02*; 0.01*; 0.12; 0.06	1.03	0.34	0.89
$\Sigma_7\text{OCPs}^a$	~ age + $\delta^{13}\text{C}$ + Loc + Yr + Loc:Yr	-5.00	-0.01	-0.36	0.91	0.13	-0.80	0.07; <0.01*; <0.01*; 0.62; 0.03*	0.00	0.37	0.91
	~ $\delta^{13}\text{C}$ + Loc + Yr + Loc:Yr	-5.71	-0.35	1.07	0.28	-0.98		<0.01*; <0.01*; 0.23; <0.01*	0.15	0.37	0.88
$\Sigma_5\text{PBDEs}$	~ age + $\delta^{13}\text{C}$	-6.71	-0.03	-0.38				<0.01*; <0.01*	0.00	0.22	0.86
	~ age + $\delta^{13}\text{C}$ + Loc + Yr + Loc:Yr	-8.39	-0.02	-0.43	0.87	0.14	-0.86	0.02*; <0.01*; 0.03*; 0.70; 0.08	0.46	0.32	0.86
	~ age + $\delta^{13}\text{C}$ + Loc	-7.07	-0.03	-0.38	0.31			<0.01*; <0.01*; 0.19	0.54	0.25	0.86
	~ age + $\delta^{13}\text{C}$ + Yr	-7.28	-0.03	-0.43	-0.31			<0.01*; <0.01*; 0.23	0.83	0.23	0.86
	~ age + $\delta^{13}\text{C}$ + Loc + Yr	-7.65	-0.03	-0.43	0.31	-0.31		<0.01*; <0.01*; 0.19; 0.22	1.34	0.27	0.86
$\Sigma_8\text{PFASs}$	~ age + Loc + Yr	1.66	0.02	0.54	-0.80			<0.01*; <0.01*; <0.01*	0.00	0.73	0.93

- 5 ^a Two outliers were removed from these models, $n = 68$.

Supporting information:

Plasma concentrations of organohalogenated contaminants in white-tailed eagle nestlings – the role of age and diet

Mari Engvig Løseth^{a*}, Nathalie Briels^a, Igor Eulaers^b, Torgeir Nygård^c, Govindan Malarvannan^d, Giulia Poma^d, Adrian Covaci^d, Dorte Herzke^e, Jan Ove Bustnes^f, Bjørn Munro Jensen^{a,b}, Gilles Lepoint^g, Veerle L. B. Jaspers^a

Affiliations:

^aDepartment of Biology, Norwegian University of Science and Technology (NTNU), Høgskoleringen 5, 7491 Trondheim, Norway

^bDepartment of Bioscience, Aarhus University, Fredriksborgvej 399, 4000 Roskilde, Denmark

^cNorwegian Institute for Nature Research (NINA), Høgskoleringen 9, 7034 Trondheim, Norway

^dToxicological Centre, University of Antwerp, Universiteitsplein 1, 2610 Wilrijk, Belgium

^eNorwegian Institute for Air Research (NILU), FRAM - High North Research Centre on Climate and the Environment, 9007 Tromsø, Norway

^fNorwegian Institute for Nature Research (NINA), FRAM - High North Research Centre on Climate and the Environment, 9007 Tromsø, Norway

^gLaboratoire d'Océanologie, University of Liège, 4000 Liège (Sart Tilman), Belgium

* corresponding author: mari.loseth@ntnu.no

Table S2: Overview of white-tailed eagle nestlings sampled in Smøla and Steigen (Norway), in 2015 and 2016.

	Smøla		Steigen	
	2015	2016	2015	2016
Number of nests	10	14	9	15
Number of nestlings	13	22	14	21
Number of females	7	9	8	10
Number of males	6	13	6	11

Table S3: Compounds and their concentrations in internal standards used for extraction of targeted PCBs, PBDEs, OCPs, NBFRs, PFRs, DPs and PFASs. Obtained from Løseth et al. (2019).

Internal standard	Concentrations and compounds
IS1 (POPs)	200 pg/μL PCB 143 25 pg/μL BDE 77 25 pg/μL ε-hexachlorocyclohexane (ε-HCH)
IS2 (ECs)	200 pg/μL ¹³ C-bis(2-ethylhexyl)-3,4,5,6-tetrabromophthalate (TBPH) 50 pg/μL ¹³ C-syn-dechlorane plus (DP) 50 pg/μL ¹³ C-anti-DP 1 ng/μL triphenyl phosphate (TPHP-d15) 1 ng/μL tris(chloroethyl) phosphate (TCEP-d12) 1 ng/μL tris-(1,3-dichloro-2-propyl) phosphate (TDCIPP-d15) 1 ng/μL triamyl phosphate (TAP) 2 ng/μL tri-(2-butoxyethyl) phosphate (TBOEP-d6)
IS3 (DPs)	200 pg/μL ¹³ C-DPs
IS4 (PFASs)	0.1 ng/μL ¹³ C-PFAS mix

Table S4: Recoveries of internal standards in plasma samples from white tailed eagles from Smøla and Steigen (Norway), from 2015 and 2016. Compounds not analysed are marked with “na”. Obtained from Løseth et al. (2019).

Plasma	2015		2016	
	Mean	sd	Mean	sd
CB 143	69	39	108	8
ε-HCH	53	12	79	11
BDE 77	83	9	87	10
¹³ C-HCB	na	na	102	17
¹³ C-TBPH	18	14	25	12
¹³ C-s-DP	47	13	55	10
¹³ C-a-DP	50	10	52	11
TAP	93	13	79	14
TCEP-d12	89	33	72	22
TBEP-d6	78	35	68	28
TPhP-d15	86	15	80	12
TDCPP-d15	92	15	80	11
¹³ C-PFPA	101	16	87	12
¹³ C-PFHxA	93	22	86	10
¹³ C-PFHpA	90	16	93	12
¹³ C-PFOA	88	15	87	12
¹³ C-PFDcA	81	32	89	11
¹³ C-PFUnA	77	13	84	12
¹³ C-PFDoA	59	15	83	19
¹³ C-PFHxS	90	17	87	12
¹³ C-PFOS	79	17	84	12
¹³ C-PFOA	83	17	75	9

Table S5: Targeted chlorinated compounds analysed in plasma from white-tailed eagle nestlings sampled at Steigen and Smøla (Norway) in 2015 and 2016. Only samples from 2016 were analysed for *p,p'*-DDD. PCB congeners are numbered by the IUPAC system (International Union of Pure and Applied Chemistry). Limit of quantification (LOQ) for the compounds are the same for 2015 and 2016 and are presented as ng/mL. Obtained from Løseth et al. (2019).

Organochlorinated compounds			
Group	Abbreviations	Compounds	LOQ plasma
Organo-Chlorinated Pesticides (OCPs)	OxC	<i>oxy</i> -chlordane	0.01
	TN	<i>trans</i> -nonachlor	0.01
	CN	<i>cis</i> -nonachlor	0.01
	HCB	hexachlorobenzene	0.01
	<i>a</i> -HCH	1 α ,2 α ,3 β ,4 α ,5 β ,6 β -hexachlorocyclohexane	0.01
	<i>b</i> -HCH	1 α ,2 β ,3 α ,4 β ,5 α ,6 β -hexachlorocyclohexane	0.01
	<i>g</i> -HCH	1 α ,2 α ,3 β ,4 α ,5 α ,6 β -hexachlorocyclohexane	0.02
	<i>p,p'</i> -DDT	<i>p,p'</i> -dichloro- α,α -diphenyl- β,β,β -trichloroethane	0.02
	<i>p,p'</i> -DDE	<i>p,p'</i> -dichloro-diphenyl-dichloroethylene	0.02
	2016	<i>p,p'</i> -DDD	<i>p,p'</i> -dichloro-diphenyl-dichloroethane
Polychlorinated Biphenyls (PCBs)	CB 28	2,4,4'-trichlorobiphenyl	0.05
	CB 49	2,2',4,5'-tetrachlorobiphenyl	0.05
	CB 52	2,2',5,5'-tetrachlorobiphenyl	0.05
	CB 74	2,4,4',5-tetrachlorobiphenyl	0.05
	CB 95	2,2',3,5',6-pentachlorobiphenyl	0.02
	CB 99	2,2',4,4',5-pentachlorobiphenyl	0.02
	CB 101	2,2',4,5,5'-pentachlorobiphenyl	0.02
	CB 105	2,3,3',4,4'-pentachlorobiphenyl	0.01
	CB 110	2,3,3',4',6-pentachlorobiphenyl	0.01
	CB 118	2,3',4,4',5-pentachlorobiphenyl	0.01
	CB 138	2,2',3,4,4',5'-hexachlorobiphenyl	0.01
	CB 149	2,2',3,4',5',6-hexachlorobiphenyl	0.01
	CB 153	2,2',4,4',5,5'-hexachlorobiphenyl	0.01
	CB 156	2,3,3',4,4',5-hexachlorobiphenyl	0.01
	CB 170	2,2',3,3',4,4',5-heptachlorobiphenyl	0.01
	CB 171	2,2',3,3',4,4',6-heptachlorobiphenyl	0.01
	CB 177	2,2',3,3',4,5',6'-heptachlorobiphenyl	0.01
	CB 180	2,2',3,4,4',5,5'-heptachlorobiphenyl	0.01
	CB 183	2,2',3,4,4',5',6-heptachlorobiphenyl	0.01
	CB 187	2,2',3,4',5,5',6-heptachlorobiphenyl	0.01
CB 194	2,2',3,3',4,4',5,5'-octachlorobiphenyl	0.01	
CB 206	2,2',3,3',4,4',5,5',6-nonachlorobiphenyl	0.01	
CB 209	Decachlorobiphenyl	0.01	

Table S6: Targeted flame retardants analysed in plasma from white-tailed eagle nestlings, sampled at Steigen and Smøla (Norway) in 2015 and 2016. PBDE congeners are numbered by the IUPAC system (International Union of Pure and Applied Chemistry). Only samples from 2016 were analyzed for 2'-MeO-BDE 68 and 6'-MeO-BDE 47. Limit of quantification (LOQ) for the compounds are the same for 2015 and 2016 and are presented as ng/mL. Compounds not targeted (analyzed) are marked with "n.a". Obtained from Løseth et al. (2019).

Flame retardants			
Group	Abbreviations	Compounds	LOQ plasma
Polybrominated diphenyl ethers (PBDEs)	BDE 28	2',4,4'-tribromodiphenyl ether	0.002
	BDE 47	2,2',4,4'-tetrabromodiphenyl ether	0.002
	BDE 99	2,2',4,4',5'-pentabromodiphenyl ether	0.002
	BDE 100	2,2',4,4',6'-pentabromodiphenyl ether	0.002
	BDE 153	2,2',4,4',5,5'-hexabromobiphenyl ether	0.002
	BDE 154	2,2',4,4',5,6'-hexabromobiphenyl ether	0.004
	BDE 183	2,2',3',4,4',5',6'-heptabromodiphenyl ether	0.004
2016	2'-MeO-BDE 68	1,5-Dibromo-3-(2,4-dibromophenoxy)-2-methoxybenzene	0.004
2016	6'-MeO-BDE 47	1,5-Dibromo-2-(2,4-dibromophenoxy)-3-methoxybenzene	0.004

Table S7: Targeted compounds for per- and polyfluorinated substance analysed in plasma from white-tailed eagle nestlings, sampled at Steigen and Smøla (Norway) in 2015 and 2016. Limit of quantification (LOQ) is given as ng/mL. Results are obtained from Løseth et al. (2019). Compounds not detected are marked n.d.

Per- and polyfluorinated substances (PFASs)				
	Abbreviations	Compounds	LOQ plasma 2015	LOQ plasma 2016
Carboxylic acids	PFBA	Perfluorobutanoic acid	169.11	0.05
	PFPeA	Perfluoropentanoic acid	1.31	0.05
	PFHxA	Perfluorohexanoic acid	1.31	0.10
	PFHpA	Perfluoroheptanoic acid	1.31	0.05
	PFOA	Perfluorooctanoic acid	0.10	0.05
	PFNA	Perfluorononanoic acid	0.10	0.08
	PFDCa	Perfluorodecanoic acid	0.10	0.05
	PFUnA	Perfluoroundecanoic acid	0.20	0.08
	PFDoA	Perfluorododecanoic acid	0.20	0.08
	PFTTrA	Perfluorotridecanoic acid	0.20	0.10
	PFTTeA	Perfluorotetradecanoic acid	0.20	0.10
Sulfonamides	PFOSA	Perfluorooctanesulfonamide	23.35	0.10
Sulfonic acids	PFBS	Perfluorobutane sulfonate	169.11	0.05
	PFPS	Perfluoropentane sulfonate	n.d.	n.d.
	PFHxS	Perfluorohexane sulfonate	0.10	0.05
	PFHpS	Perfluoroheptane sulfonate	0.01	0.08
	Lin-PFOS	Linear perfluorooctane sulfonate	0.20	0.10
	Br-PFOS	Branched perfluorooctane sulfonate	0.20	0.10
	PFNS	Perfluorononane sulfonate	n.d.	0.10

Table S8: Median, min and max concentrations (ng/ml ww) of PCBs, OCPs, PBDEs and PFASs quantified in over 50 % of plasma samples from white tailed eagles from Smøla and Steigen (Norway), from 2015 and 2016. Results are obtained from Løseth et al. (2019).

	Smøla						Steigen					
	2015 <i>n</i> = 13			2016 <i>n</i> = 22			2015 <i>n</i> = 14			2016 <i>n</i> = 21		
	median	min	max	median	min	max	median	min	max	median	min	max
CB 99	0.16	0.08	0.59	0.18	0.06	1.47	0.5	0.18	4.61	0.23	0.06	0.98
CB 101	0.21	0.09	0.31	0.14	0.01	0.56	0.16	0.07	0.56	0.14	0.02	0.25
CB 105	0.08	0.04	0.3	0.11	0.04	0.79	0.26	0.1	2.59	0.14	0.04	0.66
CB 118	0.23	0.11	0.81	0.41	0.17	2.92	0.7	0.28	7.3	0.50	0.14	2.30
CB 138	0.27	0.11	1.25	1.1	0.4	10.55	0.66	0.29	5.63	1.26	0.28	8.88
CB 153	0.74	0.21	3.06	1.44	0.55	9.48	2.05	1.12	26.27	1.75	0.43	10.16
CB 156	0.02	0.01	0.11	0.06	0.02	0.43	0.07	0.03	0.8	0.07	0.02	0.54
CB 170	0.07	0.02	0.36	0.22	0.07	1.3	0.18	0.06	2.16	0.23	0.07	1.98
CB 171	0.02	0.01	0.07	0.04	0.01	0.23	0.03	0.02	0.37	0.04	0.01	0.26
CB 177	0.02	0.01	0.07	0.04	0.02	0.43	0.03	0.01	0.18	0.05	0.01	0.17
CB 180	0.17	0.04	0.84	0.7	0.2	3.55	0.45	0.13	5.29	0.65	0.19	5.89
CB 183	0.04	0.01	0.19	0.12	0.04	0.76	0.1	0.04	1.15	0.13	0.03	1.03
CB 187	0.11	0.03	0.43	0.32	0.13	2.55	0.22	0.07	1.81	0.36	0.1	1.95
CB 194	0.03	0.02	0.08	0.08	0.02	0.3	0.05	0.02	0.38	0.07	0.02	0.79
Σ₁₄PCBs	2.00	0.82	8.47	4.86	1.86	34.52	5.12	2.95	59.05	5.79	1.58	35.92
OxC	0.04	0.02	0.14	0.08	0.02	0.53	0.24	0.05	2.16	0.13	0.04	0.6
TN	0.19	0.06	0.36	0.26	0.08	0.98	0.22	0.1	1.22	0.29	0.14	0.59
CN	0.07	0.04	0.12	0.13	0.05	0.39	0.07	0.04	0.44	0.14	0.08	0.25
<i>p,p'</i> -DDE	1.21	0.56	5.23	1.2	0.56	9.47	3.95	2.18	47.61	1.45	0.48	8.64
<i>p,p'</i> -DDT	0.2	0.08	0.3	0.15	0.06	0.63	0.13	0.06	0.31	0.27	0.09	0.38
HCB	0.09	0.04	0.21	0.76	0.26	2.96	0.15	0.05	0.8	1.02	0.32	2.46
β-HCH	0.04	0.03	0.06	0.02	0.01	0.08	0.06	0.03	0.32	0.02	0.01	0.07
Σ₇OCPs	2.01	0.89	6.28	2.75	1.05	15.33	4.75	2.80	52.19	5.79	1.31	12.96
BDE 47	0.06	0.03	0.28	0.08	0.01	0.81	0.19	0.06	1.82	0.09	0.01	0.36
BDE 99	0.01	0.003	0.03	0.02	0.003	0.16	0.04	0.01	0.23	0.03	0.002	0.08
BDE 100	0.03	0.01	0.11	0.03	0.004	0.35	0.08	0.02	0.5	0.03	0.002	0.14
BDE 153	0.01	0.003	0.02	0.01	0.004	0.08	0.02	0.003	0.07	0.01	0.002	0.08
BDE 154	0.01	0.004	0.03	0.03	0.006	0.17	0.01	0.003	0.04	0.02	0.003	0.10
Σ₅PBDEs	0.10	0.06	0.46	0.16	0.05	1.51	0.34	0.1	2.64	0.23	0.03	0.73
Br-PFOS	2.23	0.55	4.20	0.65	0.29	1.49	5.38	1.85	11.70	2.12	0.72	6.83
Lin-PFOS	14.12	6.04	31.85	5.25	2.34	8.47	16.55	9.55	27.07	7.01	3.86	17.5
PFOA	0.35	0.12	0.57	0.12	0.03	0.29	0.53	0.14	1.27	0.40	0.11	0.95
PFNA	1.82	0.57	4.86	0.56	0.35	1.77	3.58	1.56	6.48	1.69	0.63	6.60
PFDCa	1.22	0.66	2.3	0.39	0.25	0.82	1.44	0.91	2.52	0.69	0.36	1.82
PFUnA	3.59	2.43	4.36	1.15	0.68	2.05	3.36	2.30	5.08	1.40	0.94	2.15
PFDoA	0.57	0.32	0.94	0.27	0.09	0.46	0.38	0.20	0.86	0.22	0.15	0.51
Σ₈PFASs	25.69	10.29	46.65	9.18	4.58	13.26	31.80	18.36	52.94	12.76	7.21	32.90

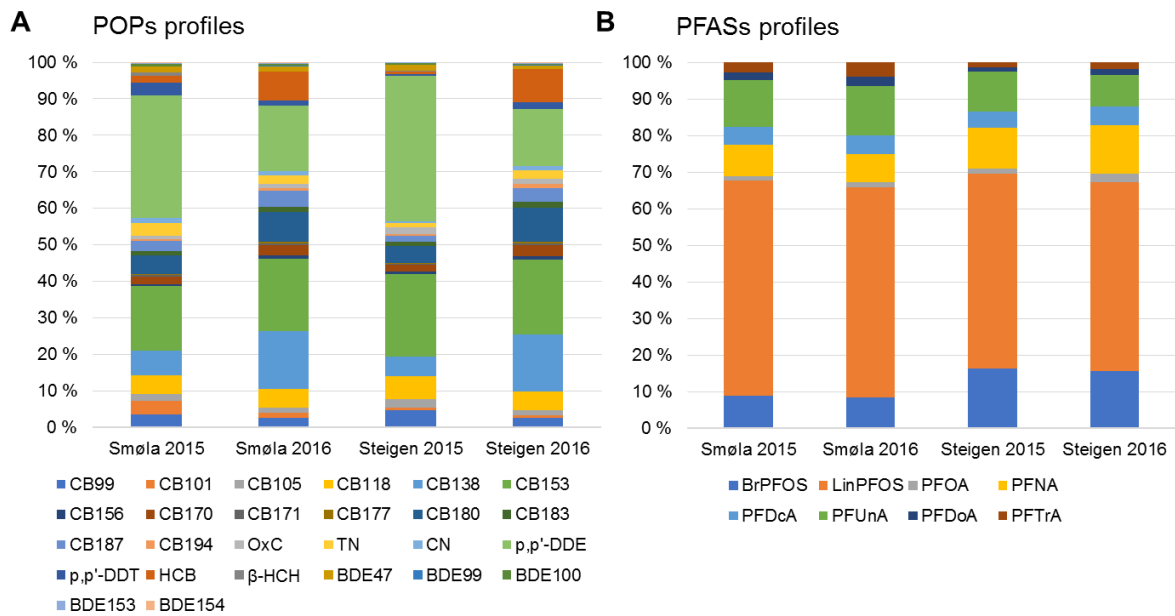


Figure S3: A) PCBs, OCPs and PBDEs and B) PFAS profiles in plasma of white-tailed eagle nestlings sampled in Smøla and Steigen (Norway), in 2015 and 2016.

Table S9: Correlations between PCBs, OCPs and PBDEs and sum of each compound group where significant correlations ($\alpha = 0.05$, Bonferroni corrected) are marked with blue colours for positive and red colours for negative correlations.

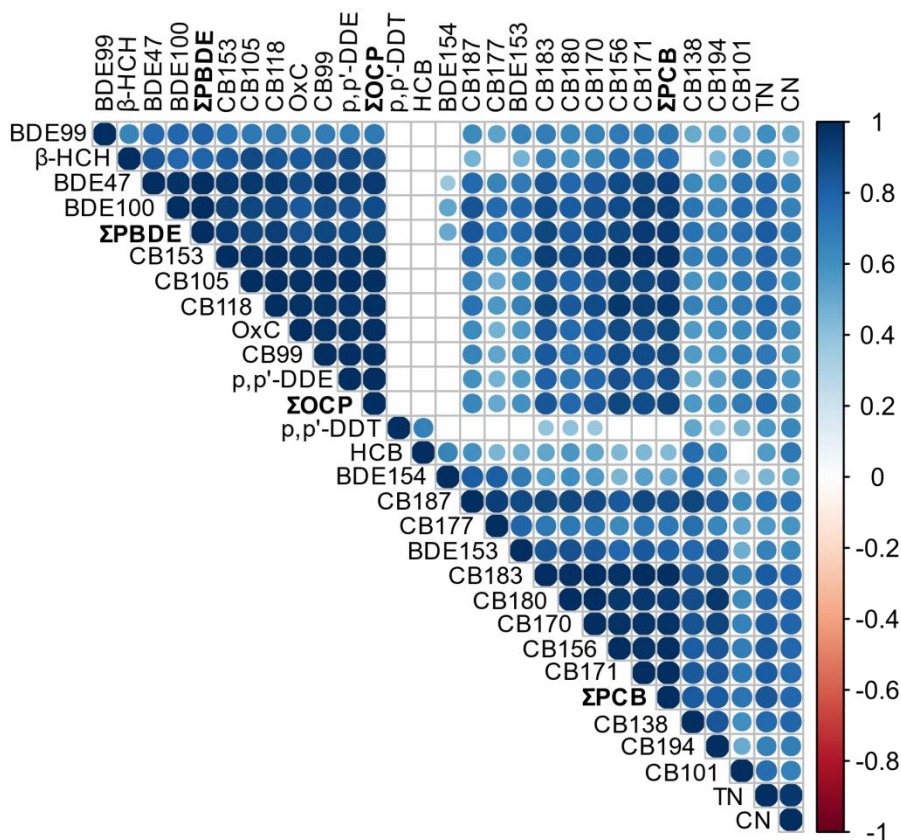
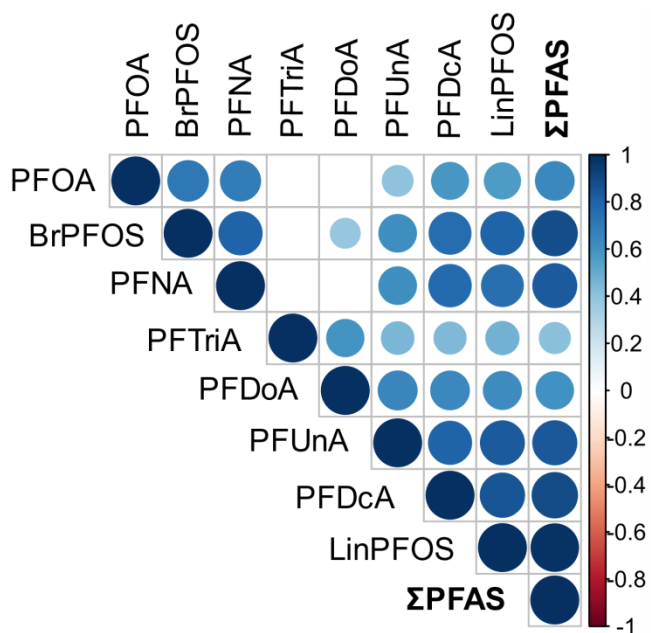


Table S10: Correlations between PFASs where significant correlations ($\alpha = 0.05$, Bonferroni corrected) are marked with blue colours for positive and red colours for negative correlations.



Body condition index

A body condition index was estimated using a standard major axis (SMA) regression to predict body mass based on wing length (Peig and Green, 2009). This regression was performed on each sex separately due to sexual dimorphism (Helander et al., 2007), and the correlation between body mass and wing length was strong and significant for both sexes (F: $r_{35} = 0.70$, $p < 0.01$, M: $r_{35} = 0.42$, $p = 0.01$). We then obtained an index of body condition for each individual by subtracting the mass predicted by the SMA regression from the observed weight. The difference between the actual weight of the individual and the predicted weight was considered the body condition index (i.e. a positive value indicates a heavier weight than would be expected for a given size of the individual). For nestlings from Smøla the BCI ranged from -0.39 – 1.42 in 2015 and from -1.30 – 0.79 in 2016, while for nestlings from Steigen BCIs ranged from -0.55 – 0.18 in 2015 and -0.33 – 0.71 in 2016.

To avoid problems with multicollinearity, we chose to include age in the models, and not body mass or BCI, as we detected significant correlations between BCI and body mass ($r_{70} = 0.64$, $p < 0.01$), between BCI and age ($r_{70} = 0.42$, $p < 0.01$) and between age and body mass ($r_{70} = 0.32$, $p < 0.01$).

Table S11: Results from lme-Anova to investigate spatial and temporal variation of the sums of each OHC group, stable isotopes ($\delta^{15}\text{N}$ and $\delta^{13}\text{C}$) and age. Significance level was set to $\alpha = 0.05$ and significant differences are marked with *.

$\Sigma_{14}\text{PCBs}$	F_(1,44)-value	p-value	$\Sigma_7\text{OCPs}$	F_(1,44)-value	p-value
Intercept	215.08	< 0.01	Intercept	183.90	< 0.01
Location	5.78	0.02*	Location	7.61	0.01*
Year	2.56	0.12	Year	0.41	0.52
Location:Year	7.58	< 0.01*	Location:Year	8.25	< 0.01*
$\Sigma_5\text{PBDEs}$			$\Sigma_8\text{PFASs}$		
Intercept	154.54	< 0.01	Intercept	2807.97	< 0.01
Location	3.27	0.08	Location	16.22	< 0.01*
Year	0.01	0.91	Year	67.89	< 0.01*
Location:Year	5.91	0.02*	Location:Year	1.19	0.28
$\delta^{15}\text{N}$			$\delta^{13}\text{C}$		
Intercept	128644.80	< 0.01	Intercept	26144.80	< 0.01
Location	15.71	< 0.01*	Location	0.07	0.80
Year	8.80	< 0.01*	Year	4.89	0.03*
Location:Year	0.06	0.80	Location:Year	0.11	0.74
Age					
Intercept	3030.87	< 0.01			
Location	3.86	0.06			
Year	2.64	0.11			
Location:Year	10.86	< 0.01*			

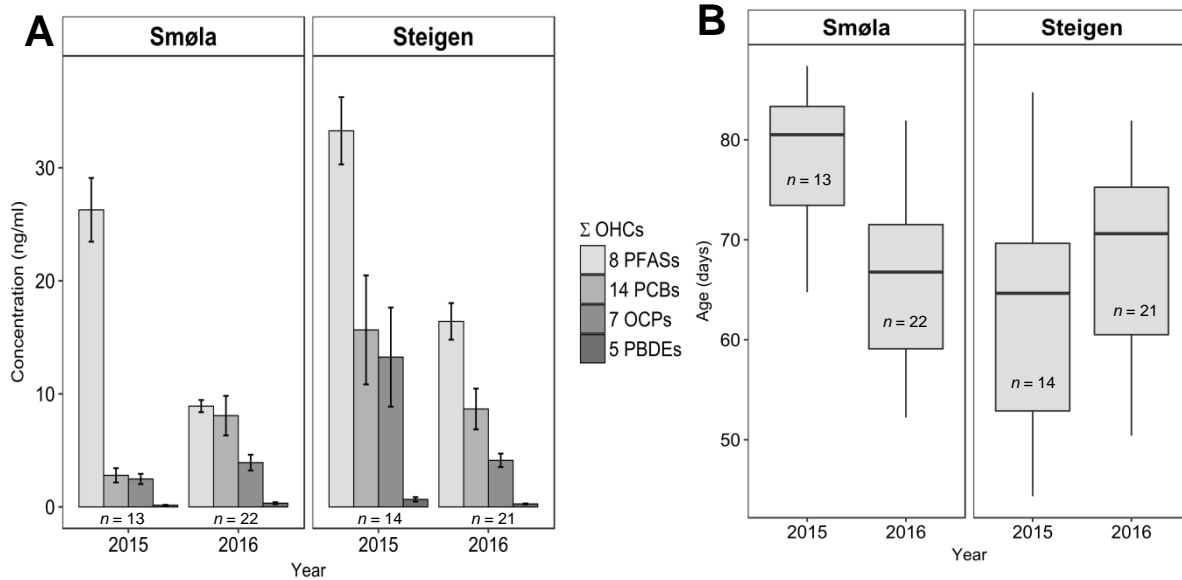


Figure S4: A) OHC concentrations (ng/ml) in plasma from white-tailed eagle nestlings sampled in Smøla and Steigen (Norway), in 2015 and 2016. B) Shows the age (days) distribution of the sampled nestlings.

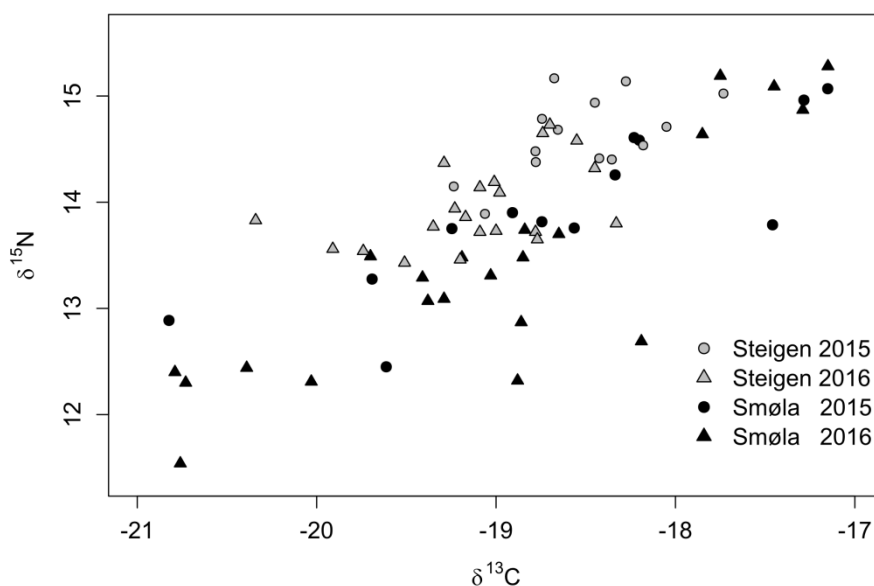


Figure S5: Stable isotope ratios of carbon ($\delta^{13}\text{C}$) and nitrogen ($\delta^{15}\text{N}$) in body feathers from white-tailed eagle nestlings, sampled in Smøla and Steigen (Norway), in 2015 and 2016.

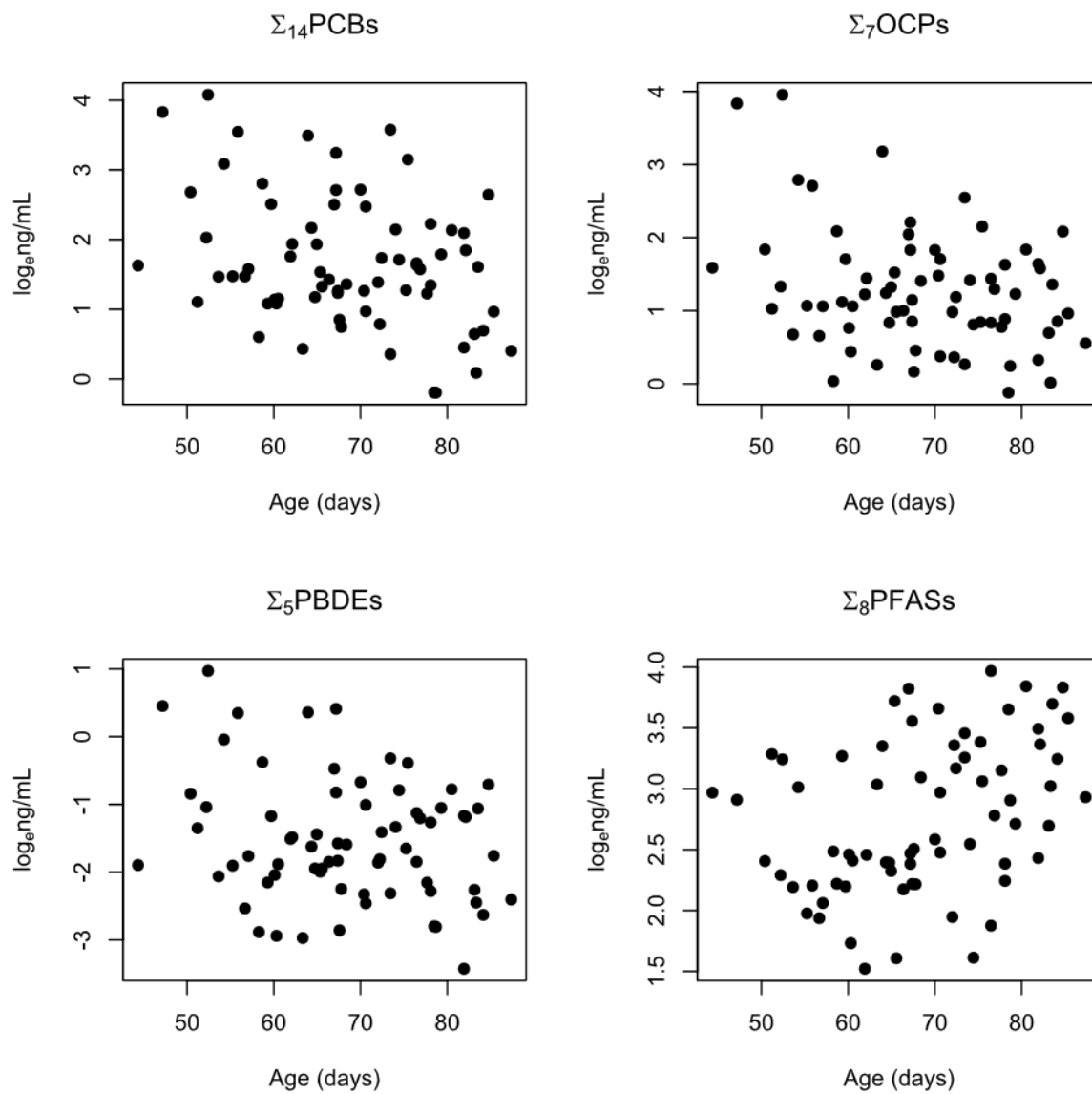


Figure S6: Plots showing the correlation between log_e concentrations of each contaminant group and age of the nestlings.

Table S12: Model selection table of all competing models for variation of $\Sigma_{14}\text{PCBs}$ in plasma from white-tailed eagle nestlings from Smøla and Steigen, sampled in 2015 and 2016. Models are ranked by increasing AICc. All models include nest as a random factor. The year variable (Yr) represents 2016 and location variable (Loc) represents Steigen

	Intercept	Age	$\delta^{13}\text{C}$	Loc	Yr	Loc:Yr	df	logLik	ΔAICc	ΔAICc	weight
m3	-3.10	-0.03	-0.36	+			6	-71.04	155.4	0.00	0.32
m4	-2.61	-0.03	-0.35				5	-72.65	156.2	0.81	0.21
m1	-3.76	-0.02	-0.35	+	+	+	8	-69.05	156.5	1.03	0.19
m2	-2.95	-0.03	-0.34	+	+		7	-70.99	157.8	2.37	0.10
m7	-2.47	-0.03	-0.34		+		6	-72.59	158.5	3.10	0.07
m6	-5.43		-0.33	+	+	+	7	-71.94	159.7	4.27	0.04
m13	3.55	-0.03		+			5	-74.96	160.8	5.43	0.02
m15	3.94	-0.03					4	-76.30	161.2	5.80	0.02
m5	2.59	-0.02		+	+	+	7	-72.71	161.2	5.81	0.02
m9	3.29	-0.03		+	+		6	-74.39	162.1	6.69	0.01
m11	3.68	-0.03			+		5	-75.75	162.4	7.02	0.01
m14	0.83			+	+	+	6	-75.20	163.7	8.31	0.01
m12	-5.02		-0.34	+			5	-76.94	164.8	9.41	0.00
m8	-4.49		-0.31	+	+		6	-76.53	166.4	10.97	0.00
m16	-4.42		-0.32				4	-79.85	168.3	12.90	0.00
m18	1.44			+			4	-80.07	168.8	13.33	0.00
m10	-3.84		-0.29		+		5	-79.38	169.7	14.28	0.00
m17	1.48				+		4	-81.30	171.2	15.79	0.00

Table S13: Model selection table of all competing models for variation of $\Sigma_7\text{OCPs}$ in plasma from white-tailed eagle nestlings from Smøla and Steigen, sampled in 2015 and 2016. Models are ranked by increasing AICc. All models include nest as a random factor. The year variable (Yr) represents 2016 and location variable (Loc) represents Steigen. Two outliers were removed from these analyses to ensure normality of the residuals (n = 68).

	Intercept	Age	$\delta^{13}\text{C}$	Loc	Yr	Loc:Yr	df	logLik	AICc	ΔAICc	weight
m1	-5.04	-0.01	-0.36	+	+	+	8	-42.51	103.50	0.00	0.38
m6	-5.75		-0.35	+	+	+	7	-43.87	103.60	0.15	0.35
m2	-4.49	-0.02	-0.36	+	+		7	-45.20	106.30	2.82	0.09
m3	-4.03	-0.01	-0.32	+			6	-46.45	106.30	2.83	0.09
m4	-3.68	-0.02	-0.32				5	-48.97	108.90	5.46	0.03
m12	-4.82		-0.31	+			5	-49.05	109.10	5.62	0.02
m7	-4.11	-0.02	-0.36		+		6	-47.90	109.20	5.72	0.02
m8	-5.24		-0.34	+	+		6	-48.47	110.30	6.86	0.01
m16	-4.47		-0.30				4	-52.58	113.80	10.35	0.00
m14	0.80			+	+	+	6	-50.97	115.30	11.86	0.00
m10	-4.81		-0.33		+		5	-52.20	115.40	11.91	0.00
m13	1.99	-0.01		+			5	-52.44	115.90	12.40	0.00
m18	1.06			+			4	-54.32	117.30	13.82	0.00
m15	2.34	-0.02					4	-54.56	117.80	14.31	0.00
m9	2.08	-0.01		+	+		6	-52.33	118.00	14.59	0.00
m11	2.43	-0.02			+		5	-54.47	119.90	16.46	0.00
m17	1.29				+		4	-57.14	122.90	19.46	0.00

Table S14: Model selection table of all competing models for variation of Σ sPBDEs in plasma from white-tailed eagle nestlings from Smøla and Steigen, sampled in 2015 and 2016. Models are ranked by increasing AICc. All models include nest as a random factor. The year variable (Yr) represents 2016 and location variable (Loc) represents Steigen.

	Intercept	Age	$\delta^{13}\text{C}$	Loc	Yr	Loc:Yr	df	logLik	AICc	ΔAICc	weight
m4	-6.71	-0.03	-0.38				5	-72.48	155.9	0.00	0.24
m1	-8.50	-0.02	-0.43	+	+	+	8	-69.00	156.4	0.46	0.19
m3	-7.09	-0.03	-0.38	+			6	-71.55	156.4	0.54	0.18
m7	-7.30	-0.03	-0.43		+		6	-71.70	156.7	0.83	0.16
m2	-7.69	-0.03	-0.43	+	+		7	-70.72	157.2	1.34	0.12
m6	-10.00		-0.43	+	+	+	7	-71.17	158.2	2.25	0.08
m12	-8.73		-0.37	+			5	-75.51	161.9	6.05	0.01
m15	0.40	-0.03					4	-76.85	162.3	6.41	0.01
m13	0.10	-0.02		+			5	-76.11	163.2	7.26	0.01
m16	-8.32		-0.36				4	-77.42	163.5	7.55	0.01
m8	-9.20		-0.40	+	+		6	-75.21	163.7	7.84	0.01
m11	0.47	-0.03			+		5	-76.81	164.6	8.66	0.00
m5	-0.49	-0.02		+	+	+	7	-74.74	165.3	9.38	0.00
m10	-8.72		-0.39		+		5	-77.20	165.3	9.44	0.00
m9	0.17	-0.03		+	+		6	-76.07	165.5	9.57	0.00
m14	-2.04			+	+	+	6	-76.54	166.4	10.51	0.00
m18	-1.68			+			4	-79.49	167.6	11.71	0.00
m17	-1.49				+		4	-80.97	170.6	14.66	0.00

Table S15: Model selection table of all competing models for variation of Σ sPFASs in plasma from white-tailed eagle nestlings from Smøla and Steigen, sampled in 2015 and 2016. Models are ranked by increasing AICc. All models include nest as a random factor. The year variable (Yr) represents 2016 and location variable (Loc) represents Steigen.

	Intercept	Age	$\delta^{13}\text{C}$	Loc	Yr	Loc:Yr	df	logLik	AICc	ΔAICc	weight
m9	1.66	0.02		+	+		6	-9.10	31.5	0.00	0.56
m2	2.22	0.02	0.03	+	+		7	-8.91	33.6	2.11	0.19
m5	1.58	0.02		+	+	+	7	-8.94	33.7	2.17	0.19
m1	2.13	0.02	0.03	+	+	+	8	-8.76	35.9	4.36	0.06
m14	3.16			+	+	+	6	-20.81	54.9	23.42	0.00
m8	3.15		0.00	+	+		6	-21.43	56.2	24.66	0.00
m11	2.16	0.02			+		5	-22.73	56.4	24.86	0.00
m6	3.29		0.01	+	+	+	7	-20.80	57.4	25.88	0.00
m7	2.77	0.02	0.03		+		6	-22.59	58.5	26.99	0.00
m17	3.30				+		4	-29.30	67.2	35.69	0.00
m10	3.42		0.01		+		5	-29.30	69.5	38.01	0.00
m3	3.55	0.02	0.14	+			6	-30.48	74.3	42.77	0.00
m13	1.00	0.02		+			5	-32.35	75.6	44.12	0.00
m4	3.88	0.02	0.13				5	-36.75	84.4	52.92	0.00
m15	1.45	0.02					4	-38.18	85	53.46	0.00
m18	2.57			+			4	-42.94	94.5	62.97	0.00
m12	4.58		0.11	+			5	-42.17	95.3	63.75	0.00
m16	4.74		0.10				4	-45.36	99.3	67.81	0.00